

Irradiation Enhances Abscopal Anti-tumor Effects of Antigen-Specific Immunotherapy through Regulating Tumor Microenvironment

Ming-Cheng Chang,^{1,2,3,6} Yu-Li Chen,^{1,6} Han-Wei Lin,⁴ Ying-Cheng Chiang,¹ Chi-Fang Chang,¹ Shu-Feng Hsieh,¹ Chi-An Chen,¹ Wei-Zen Sun,^{3,5} and Wen-Fang Cheng^{1,4,5}

¹Department of Obstetrics and Gynecology, National Taiwan University, Taipei 100, Taiwan; ²Isotope Application Division, Institute of Nuclear Energy Research, Taoyuan, Taiwan; ³Department of Anesthesiology, National Taiwan University, Taipei 100, Taiwan; ⁴Graduate Institute of Oncology, National Taiwan University, Taipei 100, Taiwan; ⁵Graduate Institute of Clinical Medicine, Medicine College of Medicine, National Taiwan University, Taipei 100, Taiwan

Ionizing radiation therapy is a well-established method of eradicating locally advanced tumors. Here, we examined whether local RT enhanced the potency of an antigen-specific DNA vaccine, and we investigated the possible underlying mechanism. Using the HPV16 E6/E7⁺ syngeneic TC-1 tumor, we evaluated the combination of CTGF/E7 vaccination with local irradiation with regard to synergistic antigen-specific immunity and anti-tumor effects. Tumor-bearing mice treated with local RT (6 Gy twice weekly) and CTGF/E7 DNA vaccination exhibited dramatically increased numbers of E7-specific CD8⁺ cytotoxic T cell precursors, higher titers of anti-E7 Abs, and significantly reduced tumor size. The combination of local RT and CTGF/E7 vaccination also elicited abscopal effects on non-irradiated local subcutaneous and distant pulmonary metastatic tumors. Local irradiation induced the expression of high-mobility group box 1 protein (HMGB-1) in apoptotic tumor cells and stimulated dendritic cell (DC) maturation, consequently inducing antigen-specific immune responses. Additionally, local irradiation eventually increased the effector-to-suppressor cell ratio in the tumor microenvironment. Overall, local irradiation enhanced the antigen-specific immunity and anti-tumor effects on local and distant metastatic tumors generated by an antigen-specific DNA vaccine. These findings suggest that the combination of irradiation with antigen-specific immunotherapy is a promising new clinical strategy for cancer therapy.

INTRODUCTION

Conventional cancer treatment modalities include surgery, radiation therapy (RT), and chemotherapy.¹ For solid cancers, surgery and RT are often non-curative due to micro-metastases that are undetectable at the time of treatment. An ideal cancer treatment would eliminate systemic tumors at multiple sites in the body and be able to distinguish between neoplastic and non-neoplastic cells.² Chemotherapy can eradicate distant metastatic tumors but cannot specifically discriminate malignant and benign/normal cells. The need for better treatment modalities is a critical issue in cancer

research. Immunotherapy, particularly antigen-specific immunotherapy, is an attractive approach for cancer treatment because it could potentially eradicate systemic cancer lesions without killing normal cells.

It is well established that ionizing RT can kill cancer cells and other cells within the tumor stroma, including endothelial cells and intratumoral lymphocytes.³ Studies have examined the use of total body or local RT in combination with immunotherapy for cancer treatment,^{4,5} and lymphopenia induction via sub-lethal total body irradiation is reportedly beneficial for tumor treatment in mice.⁶ However, total body RT is associated with immediate hematologic toxicity and long-term leukemogenic effects, and is thus considered too toxic for indolent lymphoma treatment.⁷ Most indolent lymphomas are disseminated and treated symptomatically; for instance, low-dose local RT may be applied to palliate the discomforts of localized lesions. Such application of local RT can reportedly also lead to control of some disseminated diseases, possibly because of the immunologic regulation of local RT.⁷ Local RT can induce upregulation of activation-related genes of macrophages, indicating that macrophage activation is likely induced by signals from apoptotic cells.⁸ Moreover, host immune responses could be responsible for the partial or complete remission of tumors outside the RT field, the so-called abscopal effect.⁹

Developments in cancer immunotherapy have largely focused on inducing and expanding cytotoxic and/or helper T lymphocytes, and improving immune recognition of weak antigenic determinants expressed by tumors. DNA-based cancer vaccines are a novel treatment strategy and are under investigation in numerous pre-clinical and clinical trials.^{10–13} However, few promising clinical

Received 28 February 2017; accepted 14 November 2017;
<https://doi.org/10.1016/j.ymthe.2017.11.011>.

⁶These authors contributed equally to this work.

Correspondence: Wen-Fang Cheng, Department of Obstetrics and Gynecology, National Taiwan University Hospital, Taipei 100, Taiwan.

E-mail: wenfangcheng@yahoo.com



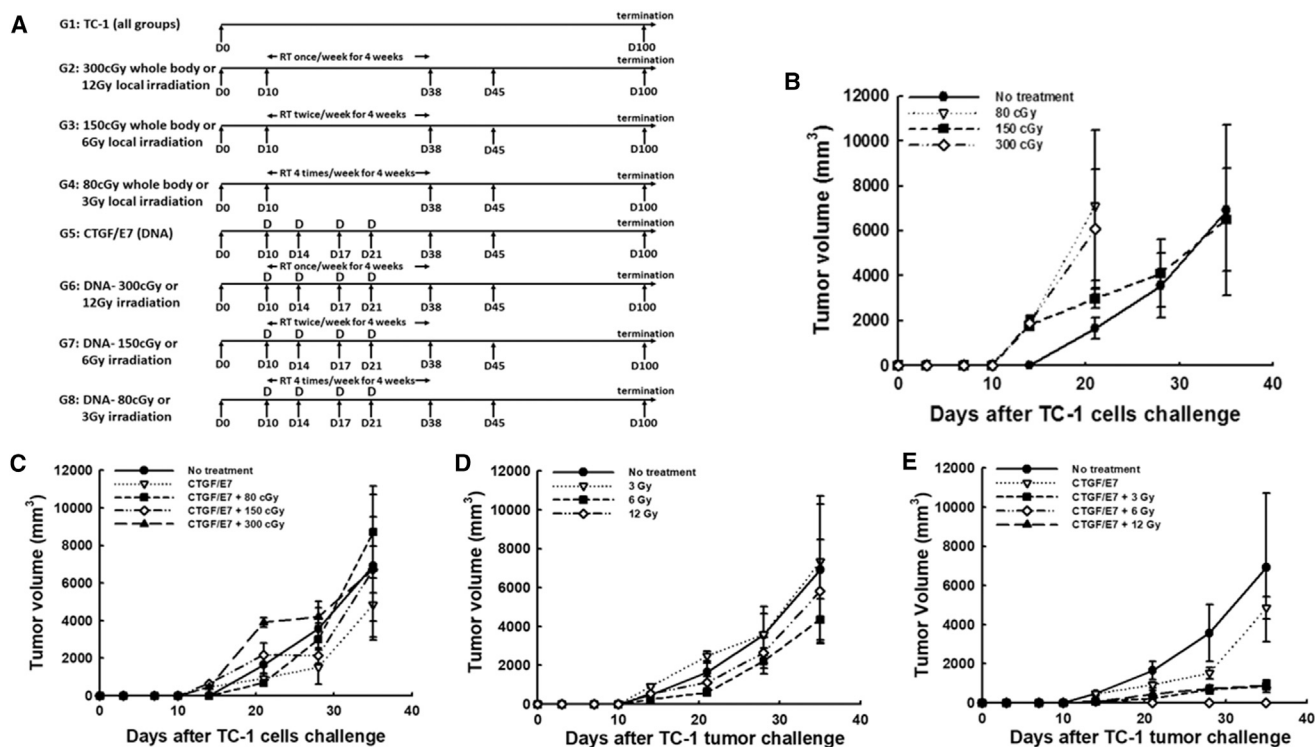


Figure 1. Therapeutic Effects of Treatment with Radiation Therapy and/or the CTGF/E7 DNA Vaccine in Mice

(A) Schematic representation of the different treatment regimens including RT and/or CTGF/E7 DNA vaccination. (B–E) Tumor volumes in TC-1-bearing mice treated with different regimens of whole-body irradiation ($n = 5$, mean \pm SD) (B), with the CTGF/E7 DNA vaccine alone or combined with different regimens of whole-body irradiation ($n = 5$, mean \pm SD) (C), with different regimens of local irradiation ($n = 5$, mean \pm SD) (D), and with the CTGF/E7 DNA vaccine alone or combined with different regimens of local irradiation ($n = 5$, mean \pm SD) (E).

outcomes have been reported. Two important issues to consider are immune tolerance and host immune deficiency. In the present study, we aimed to assess whether a combination of RT and antigen-specific immunotherapy would have synergistic effects representing an improvement over RT or immunotherapy alone. We also evaluated possible mechanisms underlying the immunotherapeutic effects of the combination of RT and antigen-specific immunotherapy.

RESULTS

Whole-Body Irradiation Combined with CTGF/E7 DNA Vaccination Did Not Generate Potent Therapeutic Anti-tumor Effects in Tumor-Bearing Mice

Tumor size did not differ significantly in tumor-bearing mice between whole-body irradiation and untreated groups (Figure 1B). Moreover, mice treated with whole-body irradiation and the CTGF/E7 DNA vaccine did not exhibit significantly smaller tumor size (tumor volume in mm^3 at day 35 [D35]) compared with other treatment groups: no treatment, $6,914.5 \pm 3,788.6$; CTGF/E7 DNA alone, $4,846.8 \pm 1,885.3$; CTGF/E7 + 80 cGy, $8,702.6 \pm 2,446.7$; CTGF/E7 + 150 cGy, $6,720.5 \pm 1,245.9$; CTGF/E7 + 300 cGy, $6,741.3 \pm 2,766.9$ ($p = 0.45$, one-way ANOVA) (Figure 1C).

Local Irradiation Combined with the CTGF/E7 DNA Vaccine Generated More Potent Anti-tumor Effects Than Local Irradiation or CTGF/E7 DNA Vaccine Alone

Tumor sizes were similar between untreated mice and those treated with local irradiation alone ($p = 0.15$; Figure 1D). However, mice that received local irradiation combined with the CTGF/E7 DNA vaccine exhibited significantly smaller tumor sizes (tumor volume in mm^3 at D35) compared with the CTGF/E7 DNA vaccine group: CTGF/E7 + 3 Gy, 850.6 ± 316.0 ; CTGF/E7 + 6 Gy, 0.0 ± 0.0 ; CTGF/E7 + 12 Gy, 889.4 ± 230.8 ; CTGF/E7 alone, $6,914.5 \pm 3,788.6$ ($p < 0.001$, one-way ANOVA) (Figure 1E). The smallest tumor size was found in mice treated with local irradiation (6 Gy/fraction, twice per week) along with the CTGF/E7 DNA vaccine.

Local Irradiation Combined with the CTGF/E7 DNA Vaccine Promoted Greater Numbers of Antigen-Specific CD8⁺ Cytotoxic T Lymphocytes and Higher Anti-E7 Ab Titers

Among tumor-bearing mice treated with whole-body irradiation, increased fractional irradiation dose was associated with decreased percentages of CD4⁺ lymphocytes ($p < 0.001$, one-way ANOVA) and CD8⁺ lymphocytes ($p = 0.002$, one-way ANOVA) among splenocytes (Figure S1). This supports that local RT might be a more appropriate method to use in combination with immunotherapy, including

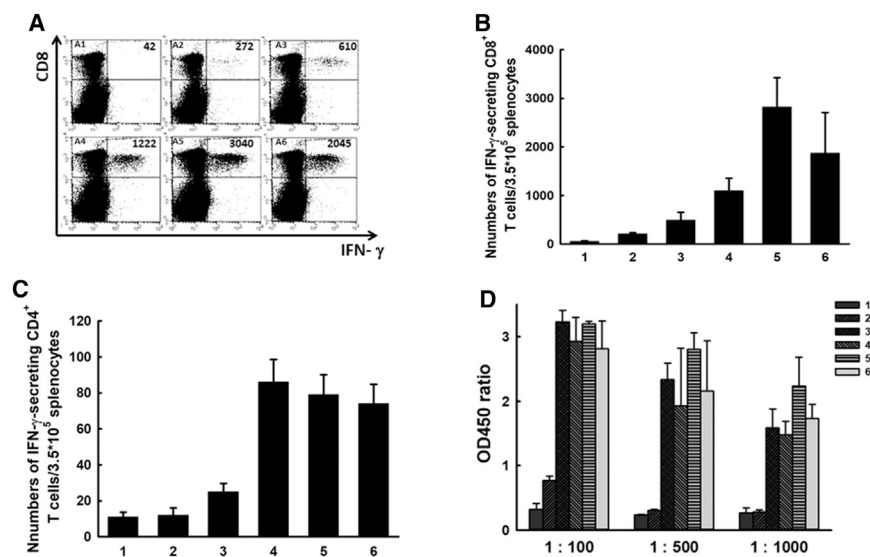


Figure 2. Antigen-Specific Immune Responses to Local Irradiation with or without the CTGF/E7 DNA Vaccine

(A) Representative figures of flow cytometry analysis of E7-specific IFN- γ -secreting CD8⁺ cytotoxic T cell precursors in the various experimental groups: A1, no treatment; A2, 6-Gy local radiation therapy (RT); A3, CTGF/E7; A4, CTGF/E7 + 3-Gy RT; A5, CTGF/E7 + 6-Gy RT; and A6, CTGF/E7 + 12-Gy RT (n = 5 per group). (B) Bar figures indicating the number of E7-specific IFN- γ -secreting CD8⁺ T cells in various experimental groups: 1, no treatment; 2, 6-Gy local RT; 3, CTGF/E7; 4, CTGF/E7 + 3-Gy RT; 5, CTGF/E7 + 6-Gy RT; and 6, CTGF/E7 + 12-Gy RT (n = 5 per group). Data are shown as mean \pm SD. (C) Bar figures indicating the number of E7-specific IFN- γ -secreting CD4⁺ cytotoxic T cell precursors in the various experimental groups: 1, no treatment; 2, 6-Gy local RT; 3, CTGF/E7; 4, CTGF/E7 + 3-Gy RT; 5, CTGF/E7 + 6-Gy RT; and 6, CTGF/E7 + 12-Gy RT (n = 5 per group). Data are shown as mean \pm SD. (D) Anti-E7 Abs detected by ELISA in the various experimental groups: 1, no treatment; 2, 6-Gy local RT; 3, CTGF/E7; 4, CTGF/E7 + 3-Gy RT; 5, CTGF/E7 + 6-Gy RT; 6, CTGF/E7 + 12-Gy RT (n = 5 per group). Data are shown as mean \pm SD.

DNA vaccines. Figure 2A shows representative figures of E7-specific CD8⁺ cytotoxic T cell precursors analyzed 7 days after the last vaccination in various experimental groups. Compared with the other groups, the mice treated with the CTGF/E7 DNA vaccine plus local irradiation with 6 Gy exhibited the greatest number of E7-specific IFN- γ -secreting CD8⁺ T cell precursors: CTGF/E7 + 3 Gy, 1,097.5 \pm 256.3; CTGF/E7 \pm 6 Gy, 2,821.5 \pm 603.9; CTGF/E7 + 12 Gy, 1,871.5 \pm 832.7; CTGF/E7 alone, 491.0 \pm 162.8 (p = 0.01, one-way ANOVA) (Figure 2B). Groups that received the CTGF/E7 DNA vaccine plus local irradiation, independent of dose, showed greater numbers of E7-specific IFN- γ -secreting CD8⁺ T cell precursors compared with the group treated with the CTGF/E7 DNA vaccine alone (p < 0.001, one-way ANOVA; Figure 2B). However, fewer E7-specific CD4⁺ T cell precursors were detected in groups treated with local irradiation and/or the CTGF/E7 DNA vaccine (Figure 2C). Moreover, mice treated with the CTGF/E7 DNA vaccine alone or in combination with local irradiation showed an increase only in the numbers of E7-specific IFN- γ -secreting CD8⁺ T cells (Figure S2).

We further evaluated the antigen-specific humoral immunity generated by local irradiation and/or the antigen-specific DNA vaccine. Tumor-bearing mice were administered the DNA vaccine and/or local irradiation, and sera were collected at specific intervals for analysis of anti-E7 Abs. The group treated with the CTGF/E7 DNA vaccine plus 6-Gy local irradiation exhibited higher anti-E7 Ab titers compared with the other groups (p = 0.03, one-way ANOVA; Figure 2D).

Local 6-Gy Irradiation Twice per Week Combined with the CTGF/E7 DNA Vaccine Generated More Potent Abscopal Anti-tumor Effects in Mice

Mice that received local irradiation alone and untreated mice showed similar distant tumor sizes of left hind legs (tumor volume in mm³

at D35): 0 Gy, 6,575.0 \pm 2,302.9; 3 Gy, 5,462.5 \pm 2,139.2; 6 Gy, 4,687.6 \pm 2,278.8; 12 Gy, 6,876.8 \pm 2,443.9 (p = 0.55, one-way ANOVA) (Figure 3A). On the other hand, mice that received local irradiation plus the CTGF/E7 DNA vaccine had smaller distant tumors compared with mice treated with the CTGF/E7 DNA vaccine alone (Figure 3B). Mice treated with 6-Gy local irradiation plus the CTGF/E7 DNA vaccine had the smaller distant tumors at D35 (2.2 \pm 0.09 mm³) compared with mice treated with the DNA vaccine plus 3-Gy local irradiation (110.3 \pm 10.3 mm³) or 12-Gy local irradiation (124.1 \pm 36.1 mm³; p < 0.001, one-way ANOVA) (Figure 3C).

Local Irradiation Combined with the CTGF/E7 DNA Vaccine Controlled Pulmonary Metastatic Tumors in Mice

Figure 3D shows representative figures of pulmonary tumor nodules in the various experimental groups. The mean number of pulmonary nodules in the mice treated with 6-Gy local irradiation plus the CTGF/E7 DNA vaccine (6.2 \pm 4.6) was lower than in the other groups (no treatment, 108.2 \pm 23.3; CTGF/E7 DNA alone, 95.2 \pm 16.5; 6-Gy irradiation alone, 87.5 \pm 22.2; p < 0.001, one-way ANOVA; Figure 3E). Mice having pulmonary metastatic nodules treated with 6-Gy local irradiation plus the CTGF/E7 DNA vaccine also exhibited significantly longer survival than the other three groups (p < 0.001, log-rank test) (Figure 3F).

Local Irradiation Combined with the CTGF/E7 DNA Vaccine Enhanced the Number of Infiltrating CD8⁺ Cytotoxic T Lymphocytes within the Index and Distant Tumors

Figure 4A shows representative figures of infiltrating leukocytes within the index tumors of various experimental groups, visualized by H&E staining. The groups treated with the CTGF/E7 DNA vaccine plus local irradiation with 6 or 12 Gy exhibited higher numbers of infiltrating leukocytes compared with the other groups (Figure 4A).

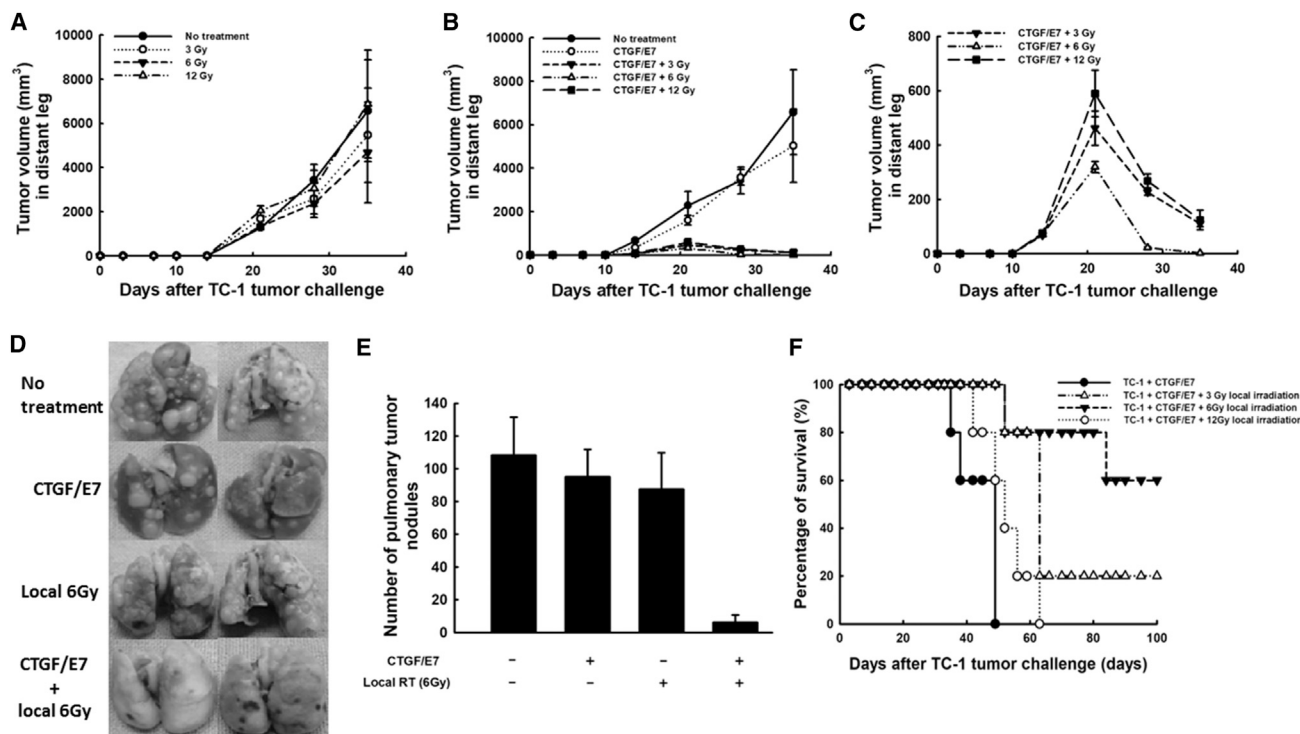


Figure 3. Abscopal Effects of Local Irradiation Plus the CTGF/E7 DNA Vaccine on Distant Tumors of the Contralateral Leg without Irradiation or Pulmonary Metastatic Tumors

(A) Volumes of distant tumors from the contralateral leg of mice treated with local irradiation on the index tumor of the right hind leg ($n = 5$ per group). Data are shown as mean \pm SD. (B) Volumes of distant tumors from the contralateral leg of mice treated with the CTGF/E7 DNA vaccine alone or combined with local irradiation on the index tumor of the right hind leg ($n = 5$ per group). Data are shown as mean \pm SD. (C) Magnification of the distant tumor volumes from the contralateral leg of mice treated with DNA vaccine combined with local irradiation on the index tumor of the right hind leg ($n = 5$ per group). Data are shown as mean \pm SD. (D) Representative figures of pulmonary metastatic tumors from mice treated with local irradiation on the index tumor of the right hind leg and/or the CTGF/E7 DNA vaccine ($n = 5$ per group). (E) Bar figure indicating the numbers of pulmonary metastatic tumors in mice treated with local irradiation on the index tumor of the right hind leg and/or the CTGF/E7 DNA vaccine ($n = 5$ per group). Data are shown as mean \pm SD. (F) Survival curves of mice having pulmonary metastatic nodules treated with local irradiation on the index tumor of the right hind leg and/or the CTGF/E7 DNA vaccine ($n = 5$ per group).

Figure 4B shows representative figures of infiltrating CD8⁺ cytotoxic lymphocytes within the index tumors of various groups, visualized by immunofluorescence staining. Mice treated with the CTGF/E7 DNA vaccine plus 6-Gy local irradiation exhibited the highest number of infiltrating CD8⁺ cytotoxic lymphocytes compared with the other groups (Figure 4B). Mice treated with the CTGF/E7 DNA vaccine plus 6-Gy local irradiation also exhibited other kinds of infiltrating immunocytes within the tumor microenvironment, including macrophages (Figure S3A), neutrophils (Figure S3B), B lymphocytes (Figure S3C), and regulatory T cells (Tregs) (Figure S3D).

The percentage of intra-tumoral CD8⁺ cytotoxic T lymphocytes within the index leg was highest in the group treated with the CTGF/E7 DNA vaccine plus 6-Gy local irradiation ($6.1\% \pm 0.6\%$) compared with the other groups (CTGF/E7 DNA alone, $4.5\% \pm 0.8\%$; 3-Gy local irradiation plus CTGF/E7 DNA vaccine, $4.6\% \pm 0.66\%$; 12-Gy local irradiation plus CTGF/E7 DNA vaccine, $3.9\% \pm 0.2\%$; $p = 0.004$, one-way ANOVA; Figure 4C). Moreover, the groups treated with the CTGF/E7 DNA vaccine plus 3-Gy local

irradiation or with the CTGF/E7 DNA vaccine alone exhibited significantly higher percentages of CD8⁺ cytotoxic T lymphocytes compared with the group treated with 12-Gy local irradiation plus the CTGF/E7 DNA vaccine ($p = 0.04$, one-way ANOVA). The percentage of CD8⁺ cytotoxic T lymphocytes did not significantly differ between the groups treated with 12-Gy local irradiation with or without the CTGF/E7 DNA vaccine ($p = 0.49$, one-way ANOVA).

We further evaluated the percentages of infiltrating CD8⁺ cytotoxic T lymphocytes within the distant tumors from the various experimental groups. As shown in Figure 4D, we found higher percentages of CD8⁺ cytotoxic T lymphocytes in the groups treated with the CTGF/E7 DNA vaccine plus local irradiation with 3 ($5.8\% \pm 0.68\%$) or 6 Gy ($5.9\% \pm 0.7\%$) compared with the other groups ($p < 0.001$, one-way ANOVA). Moreover, the group treated with the CTGF/E7 DNA vaccine plus 12-Gy local irradiation ($3.0\% \pm 0.4\%$) showed a higher percentage of CD8⁺ cytotoxic T lymphocytes than the group treated with the CTGF/E7 DNA vaccine alone ($2.0\% \pm 0.4\%$; $p = 0.02$, one-way ANOVA; Figure 4D).

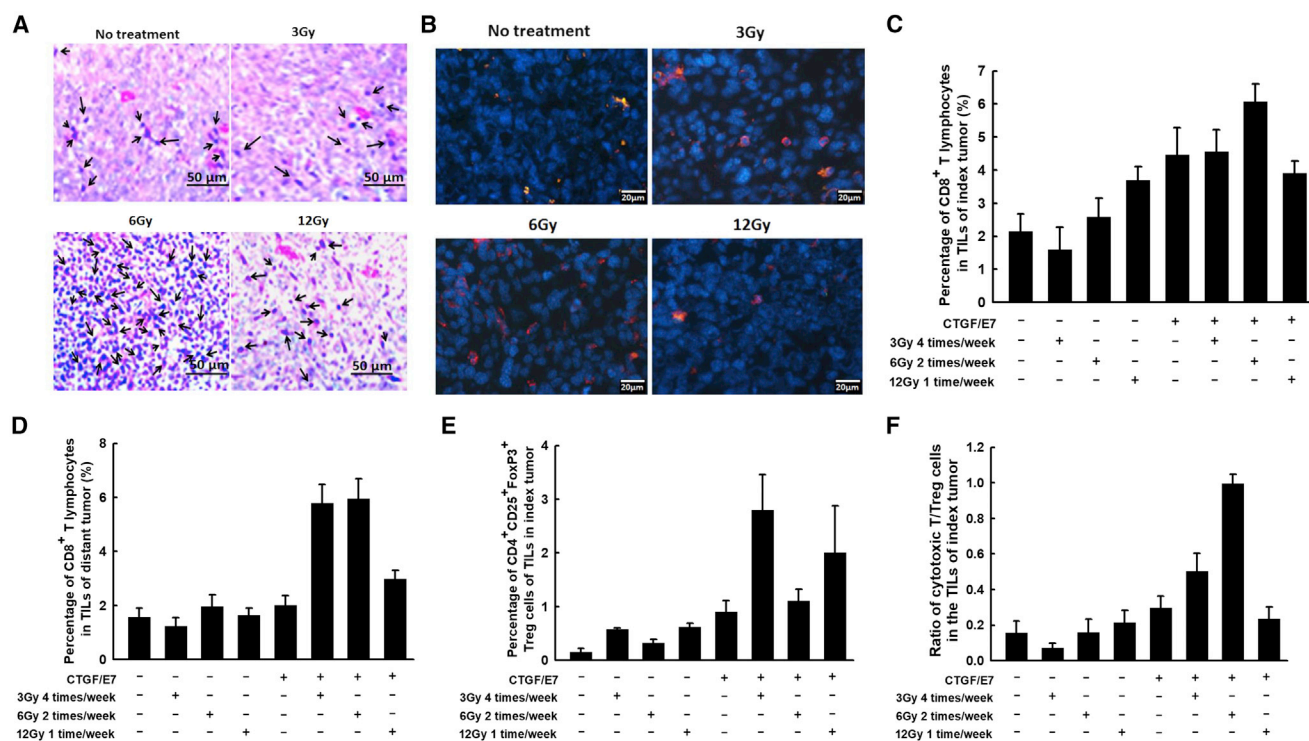


Figure 4. Immune Profiles of Effector and Suppressive T Lymphocytes among the TILs of Index and Distant Tumors from Mice Treated with Various Protocols of Local Irradiation with or without the CTGF/E7 DNA Vaccine

(A) Representative images showing H&E staining of infiltrated leukocytes in the index tumors of different experimental groups ($n = 5$ per group). Arrows indicate infiltrated leukocytes. (B) Representative images showing immunofluorescence staining of infiltrated CD8⁺ cells in the index tumors of different experimental groups ($n = 5$ per group). Blue, DAPI staining; red, CD8. (C–E) Bar figures indicating the percentages of CD8⁺ cytotoxic T lymphocytes among the TILs of the index tumors (C), the percentages of CD8⁺ cytotoxic T lymphocytes among the TILs of the distant tumors (D), and the percentages of Tregs among the TILs of the index tumors (E) from various experimental groups ($n = 5$ per group). Data are shown as mean \pm SD. (F) Bar figures indicating the ratio of cytotoxic T cells to Tregs within the index tumors from various groups ($n = 5$ per group). Data are shown as mean \pm SD.

Local Irradiation Combined with the CTGF/E7 DNA Vaccine Increased the Intra-tumoral CD8⁺-to-Regulatory T Cell Ratio within Index Tumors

Tumor-bearing mice treated with the CTGF/E7 DNA vaccine plus local irradiation with 3 ($2.8\% \pm 0.7\%$) or 12 Gy ($2.0\% \pm 0.9\%$) exhibited higher percentages of Tregs compared with the groups treated with the CTGF/E7 DNA vaccine alone ($0.9\% \pm 0.2\%$) or in addition to 6-Gy local irradiation ($1.1\% \pm 0.2\%$; $p = 0.02$, one-way ANOVA; Figure 4E). The groups did not significantly differ in the percentages of myeloid-derived suppressor cells or tumor-associated macrophages within the index tumors (data not shown).

We further evaluated the ratios of CD8⁺ cytotoxic T lymphocytes to Tregs within the index tumors of the various experimental groups. Among the groups, the mice treated with 6-Gy local irradiation plus the CTGF/E7 DNA vaccine exhibited the highest CD8⁺-to-Treg ratio (1.0 ± 0.1 ; $p < 0.001$, one-way ANOVA; Figure 4F). Moreover, the group treated with 3-Gy local irradiation plus the CTGF/E7 DNA vaccine showed a higher CD8⁺-to-Treg ratio (0.5 ± 0.1) than the group treated with the CTGF/E7 DNA alone (0.3 ± 0.1 ; $p = 0.02$, one-way ANOVA).

Local Irradiation in Tumor-Bearing Mice Led to Enhanced Infiltration of Mature Dendritic Cells by Promoting High-Mobility Group Box 1 Protein Expression in Apoptotic Tumor Cells

Figure 5A shows representative figures of terminal deoxynucleotidyl transferase (TdT)-mediated deoxyuridine triphosphate (dUTP) nick end-labeling (TUNEL) assays over time in the index tumors of the groups treated with local irradiation and/or DNA vaccination. Compared with other groups, mice that received 6-Gy local irradiation twice weekly plus the CTGF/E7 DNA vaccine exhibited the highest number of apoptotic cells at day 35 in both the index tumors (151.0 ± 8.9 ; $p < 0.001$, one-way ANOVA) and distant tumors (52.5 ± 14.7 ; $p < 0.001$, one-way ANOVA; Figure 5B).

High-mobility group box 1 protein (HMGB-1) is a key mediator in enhancing dendritic cell (DC) maturation.¹⁴ Thus, we evaluated whether irradiation enhanced DC maturation within tumors by increasing HMGB-1 expression. Figure 5C shows representative figures of HMGB-1 expression within index tumors, assessed by flow cytometry. The percentage of HMGB-1⁺ cells was highest in the group that received 6-Gy local irradiation twice weekly plus the CTGF/E7 DNA vaccine ($15.2\% \pm 2.4\%$) compared with the other

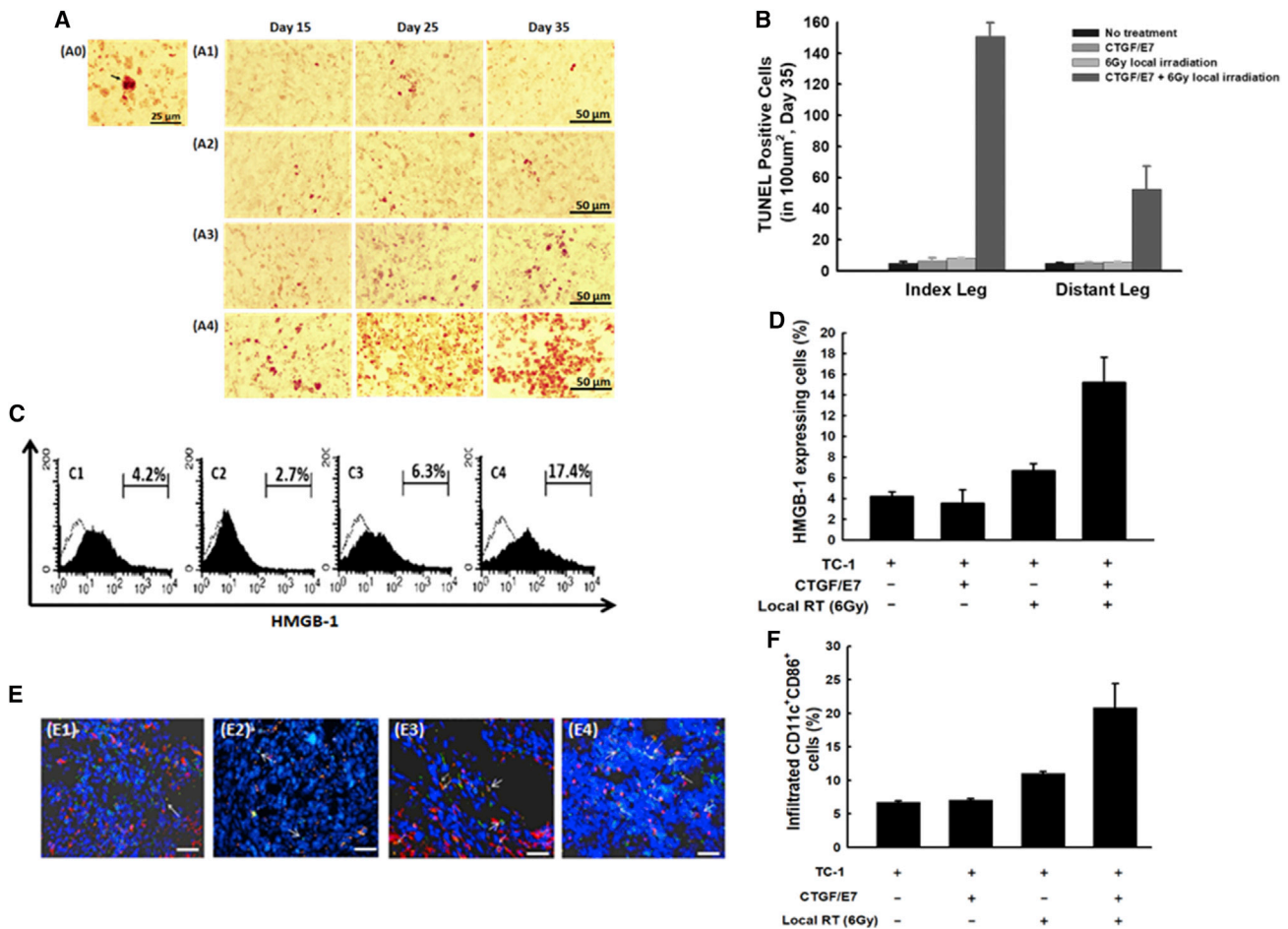


Figure 5. Apoptosis and HMGB-1 Expression within Tumor Cells, and Maturation Status of Dendritic Cells in the Tumors of Mice Treated with 6-Gy Local Irradiation and/or the CTGF/E7 DNA Vaccine

(A) Representative images showing TUNEL staining in the index tumors of mice treated with local irradiation and/or the DNA vaccine at the indicated intervals (10 × 40). A0, cell with positive TUNEL staining (arrow); A1, no treatment; A2, CTGF/E7; A3, 6-Gy local RT; A4, CTGF/E7 + 6-Gy local RT. n = 5 per group. (B) Bar figures indicating the number of TUNEL staining-positive tumor cells in the index and distant tumors from mice treated with local irradiation and/or the DNA vaccine (n = 5 per group). Data are shown as mean ± SD. (C) Representative figures showing flow cytometric analysis of HMGB-1-expressing TC-1 tumor cells of the index tumors from mice in various experimental groups: C1, no treatment; C2, CTGF/E7; C3, 6-Gy local RT; and C4, CTGF/E7 + 6-Gy local RT (n = 5 per group). (D) Bar figures indicating the HMGB-1-expressing TC-1 cells in the index tumors of various experimental groups (n = 5 per group). Data are shown as mean ± SD. (E) Representative figures showing the CD11c⁺CD86⁺ mature DCs in the index tumors of mice from various groups, visualized by immunofluorescence using a fluorescence microscope: E1, no treatment; E2, CTGF/E7; E3, 6-Gy local RT; and E4, CTGF/E7 + 6-Gy local RT. Blue, nucleus/DAPI; green, CD11c; red, CD86. n = 5 per group. (F) Bar figures indicating CD11c⁺CD86⁺ mature DCs in the index tumors of mice from various groups (n = 5 per group). Data are shown as mean ± SD.

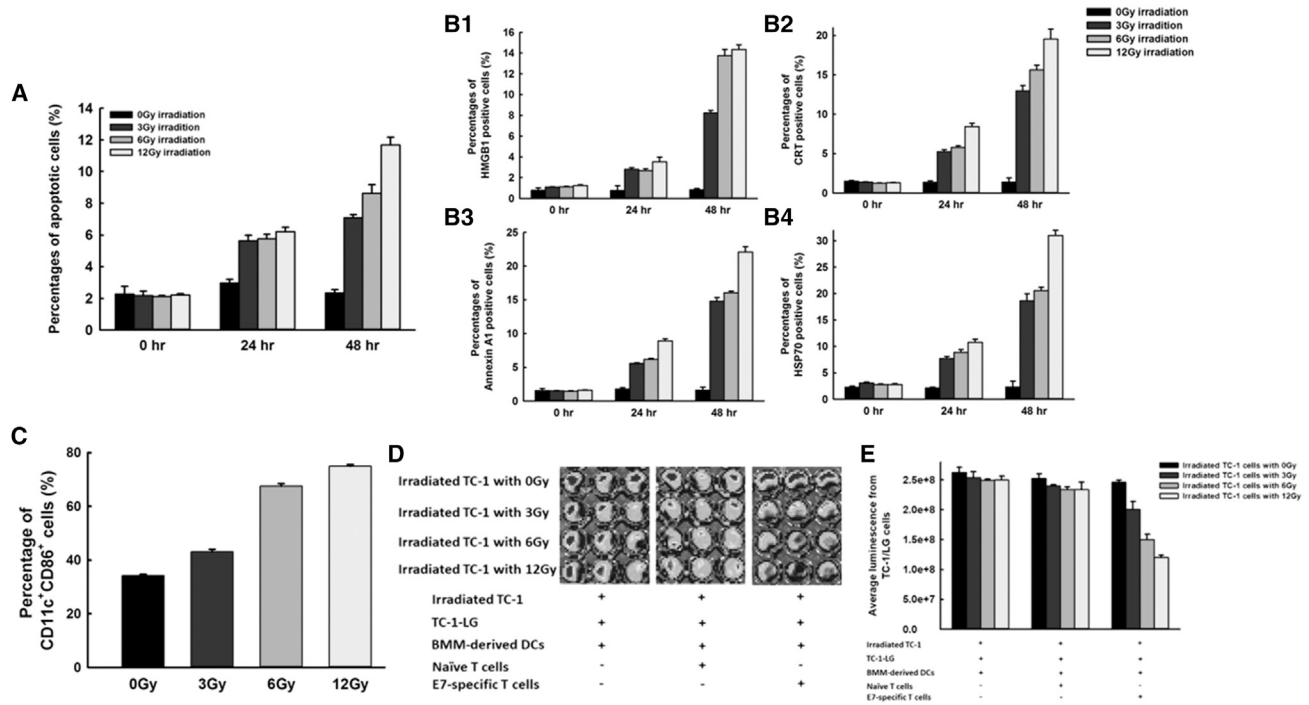
groups (no treatment, 4.2% ± 0.44%; CTGF/E7 alone, 3.5% ± 1.3%; 6-Gy local irradiation alone, 6.7% ± 0.7%; p = 0.03, one-way ANOVA; Figure 5D).

We further evaluated the maturation status of intra-tumoral DCs within the index tumors. Figure 5E shows representative images of mature DCs in the various experimental groups, visualized by immunofluorescence staining. The percentage of mature DCs within the index tumors was highest in the group that received local irradiation with 6 Gy twice weekly plus the CTGF/E7 DNA vaccine (20.8% ± 3.6%) compared with the other groups (no treatment, 6.8% ± 0.2%;

CTGF/E7 DNA vaccine alone, 7.1% ± 0.2%; 6-Gy local irradiation alone, 11.1% ± 0.2%; p < 0.001, one-way ANOVA; Figure 5F).

Irradiation of HMGB-1-Expressing Apoptotic Tumor Cells Induced Mature DCs that Enhanced Activation of Antigen-Specific Cytotoxic CD8⁺ T Lymphocytes

The apoptotic percentages of irradiated TC-1 cells correlated with the time interval after irradiation (0-Gy group: 0 hr, 2.3% ± 0.5%; 24 hr, 3.0% ± 0.2%; 48 hr, 2.4% ± 0.2%; p = 0.178, one-way ANOVA; 3-Gy group: 0 hr, 2.2% ± 0.3%; 24 hr, 5.6% ± 0.3%; 48 hr, 7.1% ± 0.2%; p < 0.001, one-way ANOVA; 6-Gy group: 0 hr, 2.1% ± 0.1%; 24 hr,



5.8% ± 0.3%; 48 hr, 8.6% ± 0.5%; $p < 0.001$, one-way ANOVA; 12-Gy group: 0 hr, 2.2% ± 0.1%; 24 hr, 6.2% ± 0.3%; 48 hr, 11.7% ± 0.5%; $p < 0.001$, one-way ANOVA; Figure 6A). Moreover, greater irradiation doses induced higher percentages of TC-1 tumor cell apoptosis with increasing post-irradiation time intervals (0-hr group: 0-Gy irradiation, 2.3% ± 0.5%; 3-Gy irradiation, 2.2% ± 0.3%; 6-Gy irradiation, 2.1% ± 0.1%; 12-Gy irradiation, 2.2% ± 0.1%; $p = 0.821$, one-way ANOVA; 24-hr group: 0-Gy irradiation, 3.0% ± 0.2%; 3-Gy irradiation, 5.6% ± 0.3%; 6-Gy irradiation, 5.8% ± 0.3%; 12-Gy irradiation, 6.2% ± 0.3%; $p < 0.001$, one-way ANOVA; 48-hr group: 0-Gy irradiation, 2.4% ± 0.2%; 3-Gy irradiation, 7.1% ± 0.2%; 6-Gy irradiation, 8.6% ± 0.5%; 12-Gy irradiation, 11.7% ± 0.5%; $p = 0.003$, one-way ANOVA).

We evaluated the expression of HMGB-1, as well as three other molecules that are characterized by damage-associated molecular patterns (DAMPs) and that can promote DC maturation: calreticulin (CRT), annexin A1, and heat shock protein 70 (HSP70).^{15,16} The percentages of HMGB-1⁺ TC-1 cells increased with an increasing time interval after irradiation (0-Gy group: 0 hr, 0.8% ± 0.2%; 24 hr, 0.8% ± 0.4%; 48 hr, 0.9% ± 0.1%; $p = 0.125$, one-way ANOVA; 3-Gy group: 0 hr, 1.1% ± 0.02%; 24 hr, 2.8% ± 0.2%; 48 hr,

8.3% ± 0.2%; $p = 0.005$, one-way ANOVA; 6-Gy group: 0 hr, 1.1% ± 0.04%; 24 hr, 2.7% ± 0.2%; 48 hr, 13.8% ± 0.6%; $p < 0.001$, one-way ANOVA; 12-Gy group: 0 hr, 1.3% ± 0.05%; 24 hr, 3.5% ± 0.4%; 48 hr, 14.4% ± 0.4%; $p < 0.001$, one-way ANOVA; Figure 6B1). Furthermore, the percentage of HMGB-1⁺ TC-1 cells increased with an increasing irradiation dose (0-hr group: 0-Gy irradiation, 0.8% ± 0.2%; 3-Gy irradiation, 1.1% ± 0.02%; 6-Gy irradiation, 1.1% ± 0.04%; 12-Gy irradiation, 1.3% ± 0.05%; $p = 0.218$, one-way ANOVA; 24-hr group: 0-Gy irradiation, 0.8% ± 0.4%; 3-Gy irradiation, 2.8% ± 0.2%; 6-Gy irradiation, 2.7% ± 0.2%; 12-Gy irradiation, 3.5% ± 0.4%; $p = 0.002$, one-way ANOVA; 48-hr group: 0-Gy irradiation, 0.9% ± 0.1%; 3-Gy irradiation, 8.3% ± 0.2%; 6-Gy irradiation, 13.8% ± 0.6%; 12-Gy irradiation, 14.4% ± 0.4%; $p < 0.001$, one-way ANOVA; Figure 6B1). The alterations of CRT⁺, annexin A1⁺, and HSP70⁺ TC-1 cells exhibited phenomena similar to those seen with HMGB-1⁺ TC-1 cells (Figure 6B2–6B4). These results indicated that expressions of DAMPs correlated with the apoptosis of irradiated TC-1 tumor cells.

The percentages of HMGB-1⁺, CRT⁺, annexin A1⁺, and HSP70⁺ TC-1 cells were higher at 48 hr than at 24 hr. Among these four molecules, HMGB-1⁺ TC-1 cells showed the highest fold-increase when

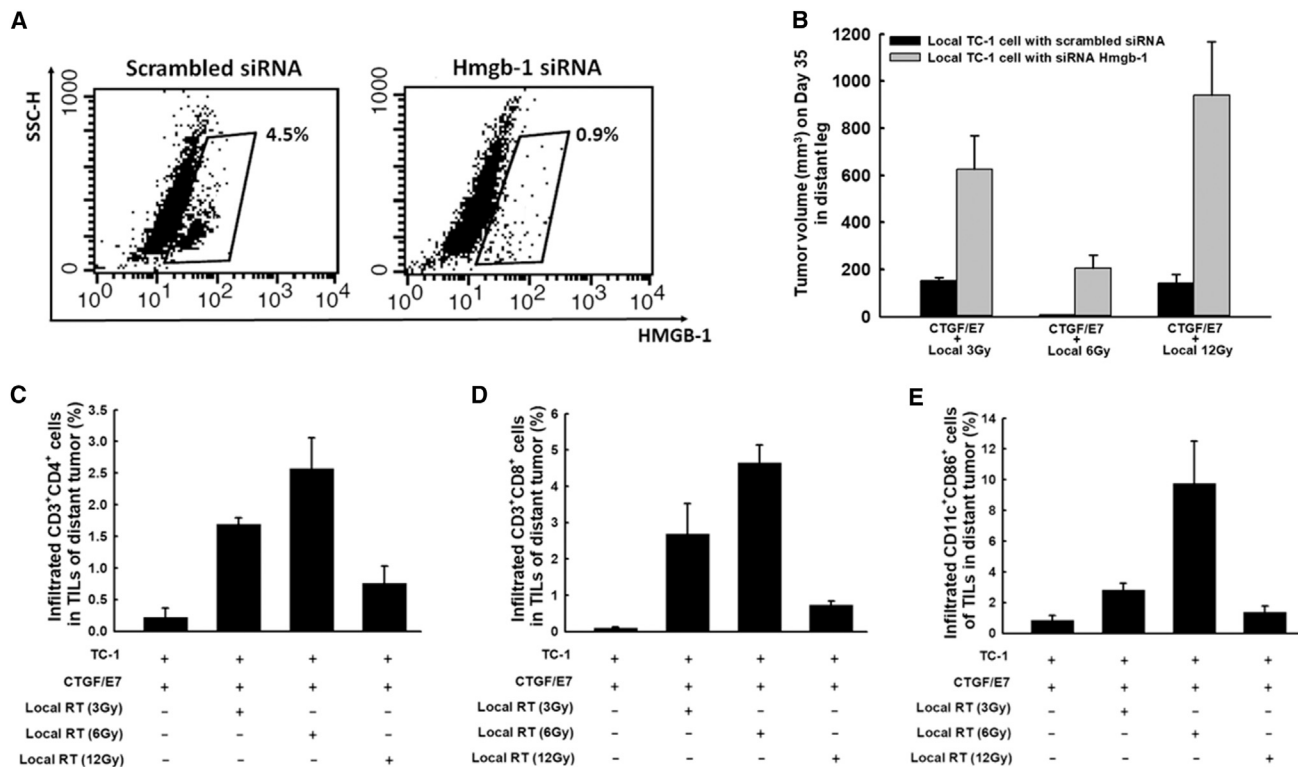


Figure 7. Abscopal Anti-tumor Effects of Local Irradiation Combined with the CTGF/E7 DNA Vaccine to Treat Index Tumors Comprising TC-1 Cells Transfected with Hmgb-1 siRNA

(A) Representative figures showing flow cytometric analysis of the efficacy of tumor cell treatment with scrambled siRNA or Hmgb-1 siRNA (n = 3 per group). (B) Bar figures indicating the volumes of distant tumors comprising wild-type TC-1 cells in mice treated with the CTGF/E7 DNA vaccine plus local irradiation to the index tumors that contained TC-1 tumor cells transfected with scrambled siRNA or Hmgb-1 siRNA (n = 5 per group). Data are shown as mean ± SD. (C–E) Bar figures indicating infiltrating CD4⁺ lymphocytes (C), infiltrating CD8⁺ lymphocytes (D), and infiltrating CD11c⁺CD86⁺ mature DCs (E) in the distant tumors of mice in various experimental groups (n = 5 per group). Data are shown as mean ± SD.

the TC-1 cells were treated with various irradiation doses (3-Gy irradiation: HMGB-1, 3.0-fold; CRT, 2.5-fold; annexin A1, 2.6-fold; HSP70, 2.4-fold; 6-Gy irradiation: HMGB-1, 5.1-fold; CRT, 2.7-fold; annexin A1, 2.6-fold; HSP70, 2.3-fold; 12-Gy irradiation: HMGB-1, 4.1-fold; CRT, 2.3-fold; annexin A1, 2.5-fold; HSP70, 2.9-fold; Figure 6B). Therefore, we selected HMGB-1 as the representative marker of DAMPs for our following knockdown experiments using short interfering RNA (siRNA).

Following co-culture with bone marrow-derived DCs, irradiated TC-1 cells showed enhanced percentages of mature DCs in a dose-dependent manner compared with non-irradiated TC-1 cells (0-Gy irradiation, 34.3% ± 0.5%; 3-Gy irradiation, 43.1% ± 1.0%; 6-Gy irradiation, 67.5% ± 0.9%; 12-Gy irradiation, 75.0% ± 0.6%; p = 0.012, one-way ANOVA; Figure 6C). Figure 6D shows representative images of the immunofluorescence of TC-1-LG tumor cells co-cultured with naive T cells or with E7-specific cytotoxic CD8⁺ T cells pulsed with bone marrow-derived monocyte (BMM)-derived DCs that were first co-cultured with irradiated TC-1 cells. Immunofluorescence did not differ between the TC-1-LG cells co-cultured with naive T cells and those co-cultured with naive T cells pulsed with irradiated

TC-1-cultured DCs (p = 0.152, one-way ANOVA; Figure 6E). Among TC-1-LG cells co-cultured with cytotoxic CD8⁺ T cells that were pulsed with irradiated TC-1-cultured DCs, immunofluorescence (p/s) was lower in the group with 12-Gy irradiated TC-1 cells ($1.2 \times 10^8 \pm 3.6 \times 10^6$) than in the other groups (0-Gy irradiation, $2.5 \times 10^8 \pm 3.3 \times 10^6$; 3-Gy local irradiation, $2.0 \times 10^8 \pm 1.3 \times 10^7$; 6-Gy local irradiation, $1.5 \times 10^8 \pm 8.8 \times 10^6$; p < 0.001, one-way ANOVA; Figure 6E).

Inhibition of HMGB-1 Could Reduce Abscopal Anti-tumor Effects

Figure 7A shows representative figures of the flow cytometric analysis of the siRNA-mediated inhibition of HMGB-1 expression in TC-1 tumor cells. Among mice treated with the CTGF/E7 DNA vaccine plus local irradiation, distant tumors at day 35 were larger among the mice with index tumors containing TC-1 cells treated with Hmgb1 siRNA compared with mice whose index tumors contained TC-1 cells treated with scrambled siRNA (CTGF/E7 + 3 Gy: Hmgb-1 siRNA, 626.5 ± 142.5 mm³ versus scrambled siRNA, 151.3 ± 13.8 mm³; p < 0.001, one-way ANOVA; CTGF/E7 + 6 Gy: Hmgb-1 siRNA, 205.7 ± 56.1 mm³ versus scrambled siRNA, 7.2 ± 1.1 mm³;

$p < 0.001$, one-way ANOVA; CTGF/E7 + 12 Gy: Hmgb-1 siRNA, $939.6 \pm 228.7 \text{ mm}^3$ versus scrambled siRNA, $143.1 \pm 35.6 \text{ mm}^3$; $p < 0.001$, one-way ANOVA; Figure 7B). These results indicated that inhibition of HMGB-1 generation in TC-1 tumor cells could decrease the abscopal anti-tumor effects of local irradiation combined with the CTGF/E7 DNA vaccine.

We further evaluated the distributions of helper, cytotoxic T lymphocytes, and DCs among the tumor-infiltrating lymphocytes (TILs) of distant tumors. The group treated with the CTGF/E7 DNA vaccine plus 6-Gy local irradiation exhibited the highest percentages of CD4⁺ helper T lymphocytes in distant tumors ($2.6\% \pm 0.5\%$) compared with the other groups (CTGF/E7 alone, $0.2\% \pm 0.1\%$; CTGF/E7 + 3-Gy local irradiation, $1.7\% \pm 0.1\%$; CTGF/E7 + 12-Gy local irradiation, $0.8\% \pm 0.3\%$; $p < 0.001$, one-way ANOVA; Figure 7C). Additionally, the percentages of CD8⁺ cytotoxic T lymphocytes (6-Gy irradiation, $4.6\% \pm 0.5\%$; $p < 0.001$, one-way ANOVA; Figure 7D) and DCs (6-Gy irradiation, $9.8\% \pm 2.8\%$; $p < 0.001$, one-way ANOVA; Figure 7E) within the distant tumors exhibited phenomena similar to those observed for the CD4⁺ helper T lymphocytes.

DISCUSSION

Whole-body irradiation can destroy tumor cells, but also bone marrow cells and even immunocytes, presenting limitations to its ability to enhance the anti-tumor effects of antigen-specific immunotherapy. Our present results showed that the anti-tumor effects of the CTGF/E7 DNA vaccine plus 4 weeks of whole-body irradiation were not better than the effects of the CTGF/E7 DNA vaccine alone (Figure 1C). When the overall duration of total body irradiation was shortened to 2 weeks, we still found a lower number of E7-specific IFN- γ -secreting CD8⁺ T cells in mice treated with the CTGF/E7 DNA vaccine plus whole-body irradiation compared with in mice treated with only the CTGF/E7 DNA vaccine (Figure S4).

Whole-body irradiation is a complex radiotherapeutic technique used to treat hematologic, oncologic, and immunologic diseases. Total body irradiation can be administered to purposefully generate an immunocompromised status to avoid rejection of donor bone marrow cells in bone marrow transplantation. This therapeutic strategy has generated good outcomes in pediatric and adult acute leukemia.¹⁷ Total body irradiation can also enhance populations of immunosuppressive cells (e.g., Tregs), regulate the expression of T cell chemokine receptors, and skew the Th1/Th2 balance toward anti-inflammatory Th2 polarization.¹⁸ Evidence further indicates that total body irradiation can destroy the immune system by decreasing the number of peripheral lymphocytes.¹⁹ In our present study, whole-body irradiation combined with an antigen-specific DNA vaccine resulted in poorer anti-tumor effects than the antigen-specific DNA vaccine alone (Figure 1C). These findings suggest that protracted whole-body irradiation alone, at the doses tested between 80 and 300 cGy weekly for 4 weeks, is not a good strategy in combination with antigen-specific immunotherapy.

Local irradiation can modify the immunosuppressive tumor environment, potentially enhancing antigen-specific immunotherapy. Our study revealed that local irradiation with an antigen-specific DNA vaccine can generate more potent anti-tumor effects than respective treatment (Figures 1D, 1E, and 3E) and is associated with more favorable ratios of effector and suppressive T lymphocytes in the tumor microenvironment (Figure 4). There are not yet any standard therapeutic regimens for the use of irradiation in combination with anti-cancer immunotherapy. With a 4-week overall course of local irradiation treatment, our survey revealed that local irradiation with 6 Gy/fraction twice per week was the most optimal dosage for enhancing the anti-tumor effects of the antigen-specific DNA vaccine when compared with 3 Gy/fraction administered four times per week and 12 Gy/fraction once per week (Figure 1E).

Possible mechanisms underlying the effects of irradiation combined with immunotherapy include enhancement of T cell infiltration²⁰ and inhibition of myeloid-derived suppressor cells (MDSCs)²¹ and Tregs.²² Our current data revealed that local irradiation enhanced effector T lymphocytes (Figures 2A and 2B) and E7-specific antibodies (Figure 2D) and decreased Tregs (Figure 4E), but not MDSCs (data not shown). The results of our previous study²³ suggest that CD8⁺ T cells would be responsible for the anti-tumor effects of local irradiation and the CTGF/E7 DNA vaccine. Depletion of host CD4⁺ T cells results in a decrease of E7-specific antibodies, but no change in the anti-tumor effects. Rather, the anti-tumor effects of the DNA vaccine depended on CD8⁺ T cells and were not inhibited by the depletion of host CD4⁺ T cells.²³ These findings suggest that elevation of the E7-specific antibody responses might not meaningfully contribute to tumor reduction in our current study.

Greater irradiation doses do not enhance the potency of antigen-specific immunotherapy. Sura et al.²⁴ reported that high-dose RT did not affect outcome or wound healing in an animal model. However, Balmanoukian et al.²⁵ reported that the severity of RT-induced leukopenia could contribute to poor survival among cancer patients. In our present study, we used fractions of the same total irradiation dose, which enhanced the anti-tumor effects of the DNA vaccine. The biweekly moderate radiation regimen (6 Gy twice per week) combined with the DNA vaccine generated more potent antigen-specific immunologic responses and anti-tumor effects (Figures 1E, 2B, and 3C) compared with groups treated with local irradiation or immunotherapy alone, or other radiation fractions (3 Gy four times per week or 12 Gy once per week) combined with the DNA vaccine. The group that received single-fraction high-dose local irradiation (12 Gy once per week) plus the DNA vaccine exhibited a significant anti-tumor effect (Figures 1E, 2B, and 3C), but also showed delayed wound healing phenomena (Figure S5). Moreover, the biweekly moderate radiation dose induced higher numbers of CD8⁺ cytotoxic T lymphocytes and further reduced the numbers of Tregs (Figures 4D and 4E). Thus, our present results suggest that the application of frequent RT administration at a lower dose (e.g., 6 Gy twice per week) in combination with antigen-specific immunotherapy could improve the therapeutic efficiency compared with the use of

antigen-specific immunotherapy alone. Further studies are needed to confirm the optimal local irradiation dose.

Treatment with a combination of local irradiation and antigen-specific immunotherapy is also an alternative therapeutic strategy against metastatic tumors. Abscopal effects are observed following antigen-specific immunotherapy combined with local irradiation, as well as with radiation alone. In our present study, local irradiation combined with the CTGF/E7 DNA vaccine induced higher numbers of E7-specific CD8⁺ cytotoxic T lymphocytes than the CTGF/E7 DNA vaccine alone (Figures 2A and 2B). Thus, the combined therapy generated more potent anti-tumor effects on local subcutaneous tumors (Figure 1E), as well as abscopal anti-tumor effects on distant and pulmonary metastatic tumors (Figures 3C and 3E). The involvement of both local and distant metastatic sites is an inherent difficulty in cancer treatment. Immunotherapy is one potential strategy for overcoming this challenge. Postow et al.²⁶ reported that irradiation combined with an immune checkpoint antibody was able to induce an abscopal effect in some patients, as observed in the current study.

Anti-tumor immunity can be improved by suppression of Tregs, which are important immunosuppressor cells in the tumor microenvironment. In our previous study, we demonstrated that the immunosuppressive cytokines interleukin-10 (IL-10) and transforming growth factor β (TGF- β) can expand the Treg population in tumors.²⁷ Our present results demonstrated that local irradiation also induced higher numbers of Tregs within tumors (Figure 4E); however, the groups treated with 3- or 6-Gy local irradiation plus the CTGR/E7 DNA vaccine showed increased ratios of effector-to-suppressive cells within the tumors (Figure 4F). Depletion of immunosuppressive cells, including Tregs or MDSCs, can reportedly reduce tumor size or tumor rejection in animal models.^{10,27,28} It will be interesting to determine whether depletion of immunosuppressive cells improves the anti-tumor effects of irradiation combined with antigen-specific immunotherapy.

DCs, especially in their mature form, stimulate potent immune responses. Functionally defective DCs are reportedly one mechanism of tumor escape from the immune system.^{29,30} Investigations have focused on strategies for restoring DC function.^{31,32} RT results in acute and local inflammatory reactions that may significantly contribute to DC infiltration into tumors.³³ It was recently demonstrated that local RT induces HMGB-1 production, which acts on DCs and improves the capacity for antigen cross-presentation to stimulate DC maturation.³⁴ Here, we found high HMGB-1 expression in apoptotic tumor cells treated with local irradiation (Figure 5D). This HMGB-1 expression promoted the generation of mature DCs with more effective presentation of the tumor antigen to effector T cells, resulting in potent anti-tumor effects.

Our *in vitro* experiments revealed that the irradiation dose correlated with the percentage of HMGB-1 expression in irradiated apoptotic TC-1 cells (Figures 6A and 6B1). Co-culturing with irradiated TC-1 cells also led to significant increases in the percentages of mature

DCs (Figure 6C). When E7-specific T cells were pulsed with DCs that had been co-cultured with irradiated TC-1 cells, their tumoricidal effects were enhanced (Figure 6D). However, these *in vitro* phenomena were not consistently observed among the *in vivo* anti-tumor effects of DNA vaccine combined with local irradiation (Figure 3C). One explanation for this discrepancy might be that the cancer microenvironment included not only tumor cells, but also non-neoplastic cells, including effective and suppressive TILs. Therefore, local irradiation could affect these TILs in addition to tumor cells *in vivo*. Among tumors irradiated with different fractional doses, there were fewer tumor-infiltrating CD8⁺ effector T cells in the 12-Gy group than in the 6-Gy group (Figure 4C). The numbers of Tregs were higher in the 12-Gy group than in the 6-Gy group (Figure 4D).

RT can also facilitate the cell surface expression of major histocompatibility complex (MHC) class I molecules.^{35,36} Radiation increases the MHC class I expression of tumor cells, which in turn can enhance their sensitivity to the killing ability of antigen-specific cytotoxic T cells.³⁵ Additionally, higher levels of MHC class I molecule expression on irradiated tumor cells can lead to increases of tumor-infiltrating CD4⁺ T, CD8⁺ T, and NK cells, which can restore host immune surveillance when combined with vaccination.³⁶ We found that radiation treatment led to significantly increased percentages of MHC class I-expressing TC-1 tumor cells compared with groups without irradiation (Figure S6). We hypothesize that this effect may partially contribute to the increased anti-tumor effects of local irradiation combined with the CTGF/E7 DNA vaccine.

The major limitation of this study is that TC-1 cells are a virus antigen (human papillomavirus [HPV] E7)-associated tumor model. Virus-associated tumors are generally immunogenic and show relatively easy induction of specific T cell responses. To investigate the treatment of non-virus-originated tumors with immunotherapy, it is necessary to explore tumor-associated antigens (TAAs), which can generate potent anti-tumor host immunity; however, this is a challenging task. Our team has developed several TAA-associated DNA vaccines, such as the CTGF/Mesothelin DNA vaccine. We found that the anti-tumor immunity against mesothelin antigen was less efficient than that against HPV E7 antigen (unpublished data). It is worth evaluating whether local irradiation can be combined to synergistically enhance the anti-tumor effects of vaccines based on other TAA-associated models.

Overall, our present examination of irradiation used in combination with antigen-specific immunotherapy in this HPV 16 E6/E7⁺ syngeneic tumor model provides a potential treatment strategy for human HPV-related malignancies. The beneficial effects of strategies based on similar mechanisms have mainly been reported in patients with lymphoid malignancies.³⁷ Administration of RT to a selected tumor site is an appropriate option for cases involving distant metastasis, especially with multiple metastasis or surgically un-resectable lesions. Such use of RT can also minimize the damage to non-neoplastic tissue. However, there remain several challenges regarding the translation of this treatment modality to human clinical applications.

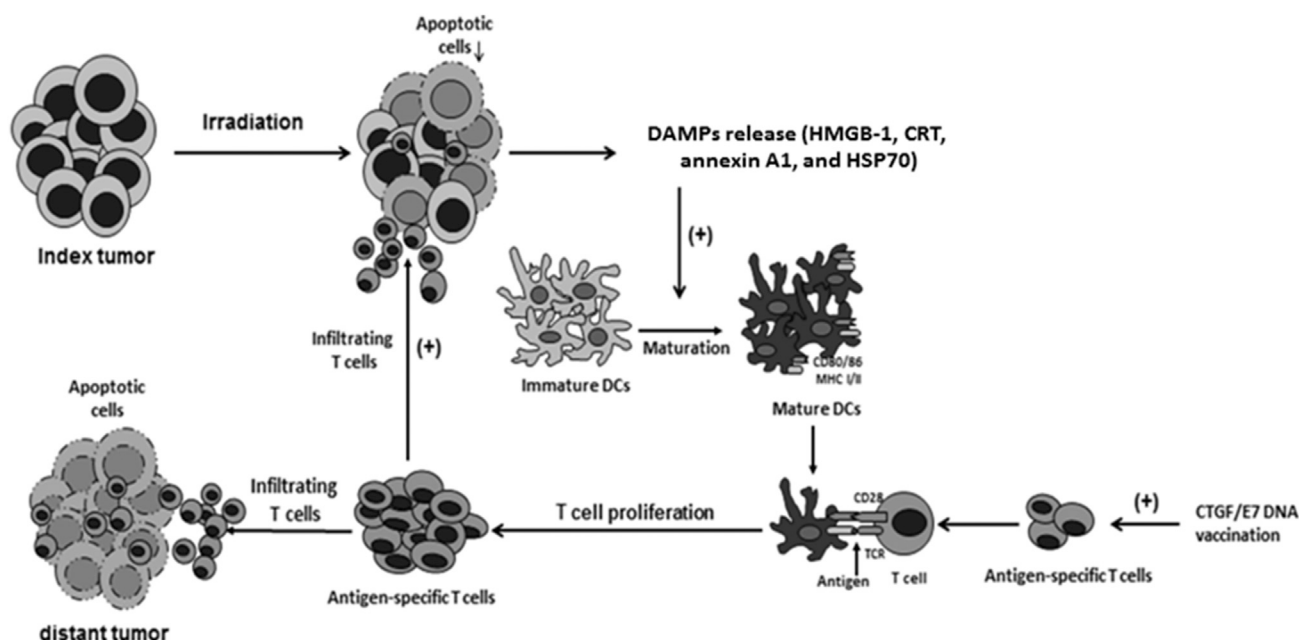


Figure 8. Schematic Diagram Showing More Potent Anti-tumor Effects of Local Irradiation Combined with Antigen-Specific DNA Vaccination

Local irradiation first induces tumor cell apoptosis, enhancing the expressions of various DAMPs, including HMGB-1. The HMGB-1 expression of apoptotic tumor cells then stimulates DC maturation. Meanwhile, the antigen-specific DNA vaccine generates antigen-specific T cells, which can be activated and their numbers can be increased through association with matured DCs. These antigen-specific T cells infiltrate both irradiated (index) and non-irradiated (distant) tumors to exert tumor-killing effects.

The key issue is the development of an effective antigen-specific DNA vaccine to enhance the host anti-tumor immunity. Moreover, the optimal dose, fraction, frequency, and timing of RT must be optimized according to disease severity, tumor size, and location. Further research is warranted to facilitate the future application of such treatment.

In Figure 8, we present a possible explanation of the enhanced anti-tumor effects of local irradiation combined with an antigen-specific DNA vaccine. In this scenario, local irradiation promotes the tumor cell apoptosis, with subsequently enhanced release of molecules characterized by DAMPs, including HMGB-1. This HMGB-1 further stimulates DC maturation. Meanwhile, DNA vaccination enhances the antigen-specific T cells, which exhibit elevated activation and proliferation through association with matured DCs. These activated antigen-specific T cells can then infiltrate into both the index and distant tumors to exert tumor-killing effects.

MATERIALS AND METHODS

Cell Line

TC-1 cell production and maintenance have been previously described.³⁸ In brief, a single-cell suspension was generated from C57BL/6 mouse lung tissue. These primary lung cells were transduced with the HPV16 E6 and E7 genes to develop immortalized lung (E6+E7) cells. Next, these cells were transduced with the ras oncogene, generating TC-1 tumor cells. To produce TC-1/Luc cells, we transduced TC-1 cells as previously described.²⁸

Mice

Six- to eight-week-old female C57BL/6J mice were purchased from National Taiwan University (Taipei, Taiwan) and bred in the animal facility of the National Taiwan University Hospital (Taipei, Taiwan). All animal procedures were performed following approved protocols that were developed in accordance with recommendations for the proper use and care of laboratory animals.

Irradiation

Mice were subjected to either local irradiation or to whole-body irradiation with a non-lethal exposure dose. Radiation was administered as previously described³⁹ with some modifications. A cobalt-60 unit (Theratronics 1000; AECL, Ottawa, ON, Canada) was used as the irradiation source.

For whole-body irradiation, mice received γ -irradiation on day 10 using various protocols: 80 cGy/fraction four times per week, 150 cGy/fraction twice per week, or 300 cGy/fraction once per week for 4 weeks. Additionally, some mice were subjected to whole-body irradiation for only 2 weeks to evaluate the impact on immune reactions in tumor-bearing mice. For local irradiation, mice received γ -irradiation at a total dosage of 12 Gy per week over 4 weeks with different fractional doses: 3 Gy/fraction four times per week (defined as the fractionated radiation dose), 6 Gy/fraction twice per week (the biweekly moderate radiation dose), or 12 Gy/fraction once per week (single-fraction high-dose radiation).

Preparation of DNA Construct and DNA Bullet

We prepared pcDNA3-CTGF/E7 as previously described.²³ In brief, CTGF was first amplified by PCR using human placenta cDNA and then cloned into the *XhoI/EcoRI* sites of the pcDNA3 vector (Invitrogen, Carlsbad, CA, USA) to generate pcDNA3-CTGF. Next, E7 was cloned into the *HindIII* sites of pcDNA3-CTGF to generate pcDNA3-CTGF/E7. The plasmid construct was confirmed by DNA sequencing. Gold particle-coated DNA bullets were prepared, and the DNA vaccine was delivered via a low pressure-accelerated gene gun (BioWare Technologies, Taipei, Taiwan) as previously described. The vaccinations were subcutaneously delivered by gene gun twice per week for 2 weeks since day 10 at the bilateral axillary and inguinal areas, based on the locations of draining lymph nodes and avoiding the subcutaneous TC-1 tumor.

In Vivo Tumor Treatment Experiments

The schematic representation of different treatment regimens was shown in Figure 1A. For experiments testing whole-body irradiation and/or the DNA vaccine, mice (five per group) were challenged with 5×10^4 TC-1 tumor cells via subcutaneous injection into the right leg on day 0. On day 10, the mice received whole-body irradiation (80 cGy/fraction four times per week, 150 cGy/fraction twice per week, or 300-cGy/fraction once per week) for 4 weeks and/or administration of 2 μ g of CTGF/E7 DNA vaccine twice per week for 2 weeks. Mice not receiving the vaccination were used as negative controls. All mice were monitored twice per week and were sacrificed 35 days after tumor challenge or when the tumor diameter reached >2.0 cm. The tumor sizes in the different groups were recorded, analyzed, and compared.

For the experiments testing local irradiation and/or the DNA vaccine, mice (five per group) were challenged with 5×10^4 TC-1 tumor cells via subcutaneous injection in the right leg on day 0. On day 10, mice received local irradiation (3 Gy/fraction four times per week, 6 Gy/fraction twice per week, or 12 Gy/fraction once per week) on the right tumor-bearing leg and/or administration of 2 μ g of CTGF/E7 DNA vaccine twice per week for 2 weeks. The mice were monitored and sacrificed as described above, and the tumor sizes were recorded, analyzed, and compared.

To evaluate abscopal anti-tumor effects, we challenged mice (five per group) with 5×10^4 TC-1 tumor cells subcutaneously injected in the right leg (index tumor) and left leg (distant tumor) on day 0. To additionally explore the role of high-mobility group box 1 protein (HMGB-1) on the abscopal anti-tumor effects, we challenged mice (five per group) via subcutaneous injection of 5×10^4 TC-1 tumor cells transduced with Hmgb1 or scrambled siRNA into the right leg (index tumor) and subcutaneous injection of 5×10^4 wild-type TC-1 tumor cells into the left leg (distant tumor) on day 0. Local irradiation was administered to the index tumor, but not the distant tumor. Mice were treated with local irradiation and/or the CTGF/E7 DNA vaccine on day 10. The mice were monitored and sacrificed as described above, and the sizes of the index and distant tumors were recorded, analyzed, and compared.

To evaluate the abscopal anti-tumor effects of irradiation and the DNA vaccine on intravenous metastatic tumors, we challenged mice (10 per group) with 5×10^4 TC-1 tumor cells subcutaneously injected into the right leg to create the index tumor, as well as intravenously injected via the tail vein to generate pulmonary metastatic tumors.¹⁰ The mice were then irradiated at the index tumor site and/or administered the CTGF/E7 DNA vaccine as described above. On day 28, five mice were sacrificed and the lungs explanted. The pulmonary tumor nodules of each mouse were evaluated and counted by researchers who were blinded to the sample identities. The remaining five mice were used for overall survival analysis, which was terminated on day 100.

ELISA for Anti-E7 Abs

Mice were challenged with TC-1 and treated with the irradiation protocol and/or CTGF/E7 DNA vaccine as described above. Serum samples were collected at day (D) 7, D14, D21, D28, and D35 after tumor challenge. A direct ELISA method was used to detect HPV E7-specific antibodies in sera, as previously described.²³

Splenocyte Preparation

Mice were challenged with TC-1 and treated with the irradiation protocol and/or CTGF/E7 DNA vaccine as described above, and the mice were sacrificed following the indicated schedules. Then, the splenocytes and antigen-specific lymphocytes were harvested and stored for further experiments as previously described.^{30,40}

Intracellular Interferon- γ Cytokine Staining and Flow Cytometric Analysis

The splenocytes obtained from the various experimental groups were incubated overnight with 1 μ g/mL MHC class I-restricted E7 peptide (amino acids [aa] 49–57), MAGE-A5 peptide (aa 5–12), or surviving peptides (aa 57–64 and 97–107) as previously described.^{23,41} We then performed cell surface marker staining with PE-conjugated anti-mouse CD4, CD8 (Pharmingen, San Diego, CA, USA) and fluorescein isothiocyanate (FITC)-conjugated anti-mouse interferon- γ (Pharmingen), followed by flow cytometry analysis as previously described.²³

Preparation of TILs from Subcutaneous or Pulmonary TC-1 Tumors

Mice were challenged with TC-1 and treated with the irradiation protocol and/or CTGF/E7 DNA vaccine as described above. Subsequently, the subcutaneous TC-1 tumors or pulmonary tissues were surgically excised, incubated in RPMI 1640 medium containing 100 U/mL penicillin and streptomycin, and then washed with PBS. Fractions of the tumors were immediately snap frozen in Tissue-Tek optimum cutting temperature (OCT) compound (Sakura Finetek, Torrance, CA, USA) or fixed with 10% formalin. Then the remaining solid tumor tissue was minced into pieces of 1–2 mm in size; immersed in serum-free RPMI 1640 medium containing 1 mg/mL collagenase D, 0.25 mg/mL DNase I (Roche, Indianapolis, IN, USA), 100 U/mL penicillin, and 100 μ g/mL streptomycin; and incubated overnight at room temperature with gentle agitation.

Next, the minced enzyme-treated tumors were passed through a 70- μm nylon filter mesh to remove undigested tissue fragments. The single-cell suspension containing TILs was washed twice in Hank's buffered salt solution ($400 \times g$ for 10 min), and viable cells were identified using trypan blue dye exclusion. The TILs were stored at -130°C for further experiments.

Flow Cytometric Analysis of Effector Lymphocytes and Immunosuppressive Tregs among Splenocytes and TILs

Splenocytes and TILs were prepared from the experimental groups of mice as described above. Effector lymphocytes were analyzed as previously described.²⁷ Tregs were identified by staining of PE-Cy5-conjugated anti-CD4, PE-conjugated anti-CD25 (PharMingen), and FITC-conjugated anti-mouse Foxp3 Abs (eBioscience, San Diego, CA, USA).²⁷

Apoptosis Detection by TdT-Mediated dUTP Nick End-Labeling Assay

TUNEL assays were performed using the TumorTACS *in situ* apoptosis detection kit (Trevigen, Gaithersburg, MD, USA). In brief, 10- μm tumor sections were mounted on silanized slides and then hydrated, fixed, and immobilized for 10 min. Next, the sections were quenched in 3% hydrogen peroxide for 5 min and then incubated with TdT enzyme for 1 hr at 37°C . Finally, the slides were stained with 3,3'-diaminobenzidine (DAB) peroxidase substrate for 5 min and mounted under coverslips. These prepared slides were examined under a light microscope, and we acquired pictures of five random fields of view per section at $\times 400$ magnification. We calculated the number of TUNEL-positive cells as apoptotic cells in each slide.

Detection of HMGB-1-Expressing Cells in Tumors by Flow Cytometric Analysis

MGB-1 is widely expressed in the nuclei of mammalian cells and plays an important role in endogenous danger signals that stimulate apoptosis.⁴² HMGB-1 also increases the immunogenicity of soluble antigens to stimulate DC function.^{43,44} To detect HMGB-1 expression in the tumor cells, we prepared single-cell suspensions from digested subcutaneous TC-1 tumors from mice in the various experimental groups, as described above. These cells were then stained with PE-conjugated anti-HMGB-1 Ab (BioLegend, San Diego, CA, USA), as previously described.⁴⁵ Finally, the cells were characterized by flow cytometry analysis as described above.

Histological and Immunohistochemical Analysis

Mice were challenged with TC-1 and treated with the irradiation protocol and/or CTGF/E7 DNA vaccine as described above. The cancerous tissues were retrieved and prepared as previously described.²⁷ Sections were stained with H&E by the National Taiwan University College of Medicine (NTUCM) laboratory animal center to observe the leukocyte distribution. Then immunohistochemistry was performed as previously described.²⁷ In brief, the sections were mounted on slides and fixed with cold methanol (-20°C) for 20 min. Then the slides were incubated with 5% fetal bovine serum (FBS) for 10 min, followed by overnight incubation at 4°C with

primary Abs, including rat anti-mouse CD8 (Abcam, Cambridge, UK), rabbit anti-mouse F4/80 (Abcam), rabbit anti-mouse Ly6g⁺ (Abcam), rat anti-mouse CD4 (Abcam), rabbit anti-mouse FOXP3 (Abcam), FITC-conjugated anti-mouse CD11cAb (Abcam), phycoerythrin (PE)-conjugated anti-mouse CD86Ab (Abcam), and PE-conjugated anti-mouse CD19 (eBioscience). The secondary Abs included donkey anti-rabbit IgG H⁺L (Alexa Fluor 594; Abcam) and donkey anti-rat IgG H⁺L (Alexa Fluor 488; Abcam). Next, the sections were counterstained with DAPI (Sigma-Aldrich, St. Louis, MO, USA), coverslipped using anti-fade mounting medium (Invitrogen, Carlsbad, CA, USA), and analyzed using a fluorescence microscope (Olympus BX51; Tokyo, Japan).

In Vitro Analysis of Irradiation-Induced TC-1 Cell Apoptosis Using Annexin V and 7-Aminoactinomycin D Staining and Flow Cytometry

To evaluate the apoptotic effects of irradiation on TC-1 tumor cells, we performed *in vitro* apoptotic assays as previously described.⁴⁶ TC-1 tumor cells were treated without or with irradiation (3, 6, or 12 Gy). Tumor cells were collected at the indicated intervals (0, 24, and 48 hr) and incubated at room temperature with FITC-conjugated annexin V and 7-aminoactinomycin D (7-AAD; BD Biosciences, Heidelberg, Germany). The cells were analyzed by flow cytometry, and apoptosis was quantified by the percentage of the population shifting to fluorescence in positivity.⁴⁷

Quantitation of TC-1 Cell Expressions of MHC Class I, HMGB-1, CRT, Annexin A1, and HSP70 following *In Vitro* Irradiation

TC-1 tumor cells were treated without or with irradiation (3, 6, or 12 Gy) and then collected at the indicated intervals (0 and 24 hr) to determine whether irradiation induced MHC class I expression. Cells were trypsinized, washed, and collected as previously described.⁴⁵ Next, the cells were stained with PE-conjugated anti-MHC class I Ab (eBioscience) and analyzed by flow cytometry.

TC-1 tumor cells were treated with or without irradiation and then collected, trypsinized, and washed as described above to analyze the expressions of HMGB-1, CRT, annexin A1, and HSP70. HMGB-1 expression was assessed as described above. To detect annexin A1, CRT, and HSP70, we incubated the cells overnight at 4°C with the respective primary Abs: rabbit anti-mouse annexin A1 (Invitrogen, Rockford, IL, USA), CRT (Thermo Scientific, Rockford, IL, USA), and HSP70 (OriGene Technologies, Rockville, MD, USA) Abs. The cells were then incubated for 1 hr at 4°C with the secondary Ab Cy5.5-conjugated goat anti-rabbit IgG-(h+l) (Bethyl, Montgomery, TX, USA).

Flow Cytometric Analysis of the Maturation Status of TILs and BMM-Derived DCs Co-cultured with Irradiated TC-1 Cells

TILs were prepared as described above. To determine whether irradiated TC-1 tumor cells stimulated DC maturation, we performed *in vitro* co-culture experiments of BMM-derived DCs and TC-1 tumor cells. The bone marrow mononuclear cells (BMMCs) were first generated as previously described.⁴⁸ In brief, BMMCs were acquired

from the femurs of C57BL/6J mice and cultured in DMEM (Invitrogen, Carlsbad, CA, USA) supplemented with 5% FBS (Hyclone, Logan, UT, USA), 10^{-2} mM 2-mercaptoethanol (2-ME; Sigma Chemicals, St. Louis, MO, USA), 2 mM L-glutamine, 1 mM vitamins, 1 mM sodium pyruvate, 1 mM non-essential amino acids, and 100 μ g/mL gentamicin (GIBCO BRL, Rockville, MD, USA). The cells were cultured for 6 days at a density of 1×10^6 cells/mL in 24-well plates (Sarstedt, Newton, NC, USA) in a total volume of 2 mL/well with 10 ng/mL recombinant murine GM-CSF (PeproTech, Rocky Hill, NJ, USA) to generate BMM-derived DCs. The TC-1 cells were irradiated, incubated, and collected as described above. BMM-derived DCs were then co-cultured for 24 hr with irradiated TC-1 cells. Non-irradiated TC-1 cells were used as a negative control. The cells and TILs were stained with FITC-conjugated anti-CD11c (eBioscience) and PE-conjugated anti-CD86 (BioLegend), and analyzed by flow cytometry as described above.

In Vitro Tumoricidal Activity of Antigen-Specific Cytotoxic CD8⁺ T Lymphocytes Activated by BMM-Derived DCs Co-cultured with Irradiated TC-1 Cells

We investigated whether E7-specific CD8⁺ cytotoxic T lymphocytes generated more potent tumor-killing effects after being co-cultured with irradiated TC-1 cultured BMM-derived DCs. We performed *in vitro* tumor-killing experiments as previously described.⁴⁸ BMM-derived DCs, irradiated TC-1 cells, and co-cultured BMM-derived DCs and irradiated TC-1 cells were prepared. BMM-derived DCs (1×10^5 cells/well) were co-cultured with irradiated TC-1 cells and subsequently co-cultured overnight with naive T cells or E7-specific CD8⁺ T cells (1:5 ratio). Next, the naive T cells or E7-specific CD8⁺ T cells were co-cultured with TC-1-LG cells (1×10^4 cells/well) in a 96-well plate for 24 hr. Luciferin (150 μ g/mL; Promega) was added to each well, and luciferase activities were measured using an IVISR Imaging system.

Hmgb-1 Knockdown in TC-1 Cells by Hmgb-1 siRNA

Hmgb-1 siRNA was designed (OriGene Technologies, Rockville, MD, USA) to suppress HMGB-1 in TC-1 tumor cells. The duplex sequence of Hmgb-1 (mouse) was SR426038A-rCrCrUrUrArUrGrArArUrCrArGrArUrArCrArArGrArGGA. An siRNA duplex carrying a 27-mer scrambled sequence was used as a negative control (OriGene Technologies). In brief, TC-1 tumor cells (2×10^5) were seeded in six-well culture plates (Corning, Corning, NY, USA) and transfected for 48 hr with 100 nM scrambled siRNA or Hmgb-1 siRNA. These TC-1 tumor cells then received irradiation with 12 Gy. At 24 hr after irradiation, the HMGB-1 expression of the TC-1 tumor cells was analyzed by flow cytometry.

Statistical Analysis

All data are expressed as mean \pm SD, representing at least two individual experiments. Data for intracellular cytokine staining and tumor treatment experiments were evaluated by ANOVA. Log-rank analysis was performed to compare the event time distributions for different mice in the survival experiments. Differences were considered significant at $p < 0.05$.

SUPPLEMENTAL INFORMATION

Supplemental Information includes six figures and can be found with this article online at <https://doi.org/10.1016/j.ymthe.2017.11.011>.

AUTHOR CONTRIBUTIONS

M.-C.C. designed and performed most experiments involving radiation therapy combined with immunotherapy, analyzed the data, and wrote the paper. Y.-L.C. designed and performed all experiments using mice, and contributed to the data analysis and paper writing and revision. H.-W.L. designed and performed the experiments for the manuscript revision. Y.-C.C. performed the experiments using cell lines. C.-F.C. performed some of the experiments using mice and cell lines. S.-F.H. performed some of the experiments using mice. C.-A.C. and W.Z.-S. participated in the early stages of the project, the experimental design, and the data analysis. W.-F.C. supervised the project, designed experiments, analyzed data, and wrote the paper.

CONFLICTS OF INTEREST

All of the authors declare that there is no conflict of interest that could be perceived as prejudicing the impartiality of the research reported.

ACKNOWLEDGMENTS

This work was partly supported by the 2nd and 7th core laboratory facilities of the Department of Medical Research of National Taiwan University Hospital. This study was also supported by grants from the Ministry of Science and Technology of Taiwan (MOST101-2314-B-002-076-MY3 and 103-2314-B-002-191-MY3). The funding agency had no role in the study design, data collection and analysis, decision to publish, or preparation of the manuscript.

REFERENCES

- Huang, S.H., Hansen, A., Rathod, S., and O'Sullivan, B. (2015). Primary surgery versus (chemo)radiotherapy in oropharyngeal cancer: the radiation oncologist's and medical oncologist's perspectives. *Curr. Opin. Otolaryngol. Head Neck Surg.* 23, 139–147.
- Palucka, A.K., and Coussens, L.M. (2016). The basis of oncoimmunology. *Cell* 164, 1233–1247.
- Mikuriya, S., and Oh'ami, H. (1983). Radiotherapy and cellular infiltration of tumor nests. *Radiat. Med.* 1, 248–254.
- Barker, C.A., and Postow, M.A. (2014). Combinations of radiation therapy and immunotherapy for melanoma: a review of clinical outcomes. *Int. J. Radiat. Oncol. Biol. Phys.* 88, 986–997.
- Formenti, S.C., and Demaria, S. (2013). Combining radiotherapy and cancer immunotherapy: a paradigm shift. *J. Natl. Cancer Inst.* 105, 256–265.
- Hellström, K.E., Hellström, I., Kant, J.A., and Tamerius, J.D. (1978). Regression and inhibition of sarcoma growth by interference with a radiosensitive T-cell population. *J. Exp. Med.* 148, 799–804.
- Ganem, G., Cartron, G., Girinsky, T., Haas, R.L., Cosset, J.M., and Solal-Celigny, P. (2010). Localized low-dose radiotherapy for follicular lymphoma: history, clinical results, mechanisms of action, and future outlooks. *Int. J. Radiat. Oncol. Biol. Phys.* 78, 975–982.
- Driessens, G., Nuttin, L., Gras, A., Maetens, J., Mieviss, S., Schoore, M., Velu, T., Tenenbaum, L., Pr at, V., and Bruyns, C. (2011). Development of a successful anti-tumor therapeutic model combining *in vivo* dendritic cell vaccination with tumor irradiation and intratumoral GM-CSF delivery. *Cancer Immunol. Immunother.* 60, 273–281.

9. Demaria, S., Ng, B., Devitt, M.L., Babb, J.S., Kawashima, N., Liebes, L., and Formenti, S.C. (2004). Ionizing radiation inhibition of distant untreated tumors (abscopal effect) is immune mediated. *Int. J. Radiat. Oncol. Biol. Phys.* 58, 862–870.
10. Chen, C.A., Ho, C.M., Chang, M.C., Sun, W.Z., Chen, Y.L., Chiang, Y.C., Syu, M.H., Hsieh, C.Y., and Cheng, W.F. (2010). Metronomic chemotherapy enhances anti-tumor effects of cancer vaccine by depleting regulatory T lymphocytes and inhibiting tumor angiogenesis. *Mol. Ther.* 18, 1233–1243.
11. Hsieh, C.Y., Chen, C.A., Huang, C.Y., Chang, M.C., Lee, C.N., Su, Y.N., and Cheng, W.F. (2007). IL-6-encoding tumor antigen generates potent cancer immunotherapy through antigen processing and anti-apoptotic pathways. *Mol. Ther.* 15, 1890–1897.
12. Cheng, W.F., Hung, C.F., Chai, C.Y., Hsu, K.F., He, L., Ling, M., and Wu, T.C. (2001). Tumor-specific immunity and antiangiogenesis generated by a DNA vaccine encoding calreticulin linked to a tumor antigen. *J. Clin. Invest.* 108, 669–678.
13. Trimble, C.L., Peng, S., Kos, F., Gravitt, P., Viscidi, R., Sugar, E., Pardoll, D., and Wu, T.C. (2009). A phase I trial of a human papillomavirus DNA vaccine for HPV16+ cervical intraepithelial neoplasia 2/3. *Clin. Cancer Res.* 15, 361–367.
14. Bianchi, M.E., and Manfredi, A.A. (2007). High-mobility group box 1 (HMGB1) protein at the crossroads between innate and adaptive immunity. *Immunol. Rev.* 220, 35–46.
15. Hernandez, C., Huebener, P., and Schwabe, R.F. (2016). Damage-associated molecular patterns in cancer: a double-edged sword. *Oncogene* 35, 5931–5941.
16. McNulty, S., Colaco, C.A., Blandford, L.E., Bailey, C.R., Baschieri, S., and Todryk, S. (2013). Heat-shock proteins as dendritic cell-targeting vaccines—getting warmer. *Immunology* 139, 407–415.
17. Hahn, T., Wall, D., Camitta, B., Davies, S., Dillon, H., Gaynon, P., Larson, R.A., Parsons, S., Seidenfeld, J., Weisdorf, D., and McCarthy, P.L., Jr. (2006). The role of cytotoxic therapy with hematopoietic stem cell transplantation in the therapy of acute lymphoblastic leukemia in adults: an evidence-based review. *Biol. Blood Marrow Transplant.* 12, 1–30.
18. Qiao, S., Ren, H., Shi, Y., and Liu, W. (2014). Allogeneic compact bone-derived mesenchymal stem cell transplantation increases survival of mice exposed to lethal total body irradiation: a potential immunological mechanism. *Chin. Med. J. (Engl.)* 127, 475–482.
19. Song, K.H., Kim, M.H., Kang, S.M., Jung, S.Y., Ahn, J., Woo, H.J., Nam, S.Y., Hwang, S.G., Ryu, S.Y., and Song, J.Y. (2015). Analysis of immune cell populations and cytokine profiles in murine splenocytes exposed to whole-body low-dose irradiation. *Int. J. Radiat. Biol.* 91, 795–803.
20. Twyman-Saint Victor, C., Rech, A.J., Maity, A., Rengan, R., Pauken, K.E., Stelekati, E., Benci, J.L., Xu, B., Dada, H., Odorizzi, P.M., et al. (2015). Radiation and dual checkpoint blockade activate non-redundant immune mechanisms in cancer. *Nature* 520, 373–377.
21. Filatenkov, A., Baker, J., Mueller, A.M., Kenkel, J., Ahn, G.O., Dutt, S., Zhang, N., Kohrt, H., Jensen, K., Dejbakhsh-Jones, S., et al. (2015). Ablative tumor radiation can change the tumor immune cell microenvironment to induce durable complete remissions. *Clin. Cancer Res.* 21, 3727–3739.
22. Persa, E., Balogh, A., Sáfrány, G., and Lumniczky, K. (2015). The effect of ionizing radiation on regulatory T cells in health and disease. *Cancer Lett.* 368, 252–261.
23. Cheng, W.F., Chang, M.C., Sun, W.Z., Lee, C.N., Lin, H.W., Su, Y.N., Hsieh, C.Y., and Chen, C.A. (2008). Connective tissue growth factor linked to the E7 tumor antigen generates potent antitumor immune responses mediated by an antiapoptotic mechanism. *Gene Ther.* 15, 1007–1016.
24. Sura, S., Yorke, E., Jackson, A., and Rosenzweig, K.E. (2007). High-dose radiotherapy for the treatment of inoperable non-small cell lung cancer. *Cancer J.* 13, 238–242.
25. Balmanoukian, A., Ye, X., Herman, J., Laheru, D., and Grossman, S.A. (2012). The association between treatment-related lymphopenia and survival in newly diagnosed patients with resected adenocarcinoma of the pancreas. *Cancer Invest.* 30, 571–576.
26. Postow, M.A., Callahan, M.K., Barker, C.A., Yamada, Y., Yuan, J., Kitano, S., Mu, Z., Rasalan, T., Adamow, M., Ritter, E., et al. (2012). Immunologic correlates of the abscopal effect in a patient with melanoma. *N. Engl. J. Med.* 366, 925–931.
27. Chen, Y.L., Chang, M.C., Chen, C.A., Lin, H.W., Cheng, W.F., and Chien, C.L. (2012). Depletion of regulatory T lymphocytes reverses the imbalance between pro- and anti-tumor immunities via enhancing antigen-specific T cell immune responses. *PLoS ONE* 7, e47190.
28. Srivastava, M.K., Zhu, L., Harris-White, M., Kar, U.K., Huang, M., Johnson, M.F., Lee, J.M., Elashoff, D., Strieter, R., Dubinett, S., and Sharma, S. (2012). Myeloid suppressor cell depletion augments antitumor activity in lung cancer. *PLoS ONE* 7, e40677.
29. Thurner, B., Haendle, I., Röder, C., Dieckmann, D., Keikavoussi, P., Jonuleit, H., Bender, A., Maczek, C., Schreiner, D., von den Driesch, P., et al. (1999). Vaccination with mage-3A1 peptide-pulsed mature, monocyte-derived dendritic cells expands specific cytotoxic T cells and induces regression of some metastases in advanced stage IV melanoma. *J. Exp. Med.* 190, 1669–1678.
30. Huang, C.T., Chang, M.C., Chen, Y.L., Chen, T.C., Chen, C.A., and Cheng, W.F. (2015). Insulin-like growth factors inhibit dendritic cell-mediated anti-tumor immunity through regulating ERK1/2 phosphorylation and p38 dephosphorylation. *Cancer Lett.* 359, 117–126.
31. Ning, Y., Xu, D., Zhang, X., Bai, Y., Ding, J., Feng, T., Wang, S., Xu, N., Qian, K., Wang, Y., and Qi, C. (2016). β -Glucan restores tumor-educated dendritic cell maturation to enhance antitumor immune responses. *Int. J. Cancer* 138, 2713–2723.
32. Hovden, A.O., Karlsen, M., Jonsson, R., Aarstad, H.J., and Appel, S. (2011). Maturation of monocyte derived dendritic cells with OK432 boosts IL-12p70 secretion and conveys strong T-cell responses. *BMC Immunol.* 12, 2.
33. Jahns, J., Anderegg, U., Saalbach, A., Rosin, B., Patties, I., Glasow, A., Kamprad, M., Scholz, M., and Hildebrandt, G. (2011). Influence of low dose irradiation on differentiation, maturation and T-cell activation of human dendritic cells. *Mutat. Res.* 709–710, 32–39.
34. Shen, X., Hong, L., Sun, H., Shi, M., and Song, Y. (2009). The expression of high-mobility group protein box 1 correlates with the progression of non-small cell lung cancer. *Oncol. Rep.* 22, 535–539.
35. Reits, E.A., Hodge, J.W., Herberts, C.A., Groothuis, T.A., Chakraborty, M., Wansley, E.K., Camphausen, K., Luiten, R.M., de Ru, A.H., Neijssen, J., et al. (2006). Radiation modulates the peptide repertoire, enhances MHC class I expression, and induces successful antitumor immunotherapy. *J. Exp. Med.* 203, 1259–1271.
36. Newcomb, E.W., Demaria, S., Lukyanov, Y., Shao, Y., Schnee, T., Kawashima, N., Lan, L., Dewynngaert, J.K., Zagzag, D., McBride, W.H., and Formenti, S.C. (2006). The combination of ionizing radiation and peripheral vaccination produces long-term survival of mice bearing established invasive GL261 gliomas. *Clin. Cancer Res.* 12, 4730–4737.
37. Park, B., Yee, C., and Lee, K.M. (2014). The effect of radiation on the immune response to cancers. *Int. J. Mol. Sci.* 15, 927–943.
38. Lin, K.Y., Guarnieri, F.G., Staveley-O'Carroll, K.F., Levitsky, H.I., August, J.T., Pardoll, D.M., and Wu, T.C. (1996). Treatment of established tumors with a novel vaccine that enhances major histocompatibility class II presentation of tumor antigen. *Cancer Res.* 56, 21–26.
39. Mole, R.H., Papworth, D.G., and Corp, M.J. (1983). The dose-response for x-ray induction of myeloid leukaemia in male CBA/H mice. *Br. J. Cancer* 47, 285–291.
40. Chang, M.C., Chen, Y.L., Chiang, Y.C., Chen, T.C., Tang, Y.C., Chen, C.A., Sun, W.Z., and Cheng, W.F. (2016). Mesothelin-specific cell-based vaccine generates antigen-specific immunity and potent antitumor effects by combining with IL-12 immunomodulator. *Gene Ther.* 23, 38–49.
41. Hofmann, U.B., Voigt, H., Andersen, M.H., Straten, P.T., Becker, J.C., and Eggert, A.O. (2009). Identification and characterization of survivin-derived H-2Kb-restricted CTL epitopes. *Eur. J. Immunol.* 39, 1419–1424.
42. Müller, S., Ronfani, L., and Bianchi, M.E. (2004). Regulated expression and subcellular localization of HMGB1, a chromatin protein with a cytokine function. *J. Intern. Med.* 255, 332–343.

43. Rovere-Querini, P., Capobianco, A., Scaffidi, P., Valentini, B., Catalanotti, F., Giazon, M., Dumitriu, I.E., Müller, S., Iannaccone, M., Traversari, C., et al. (2004). HMGB1 is an endogenous immune adjuvant released by necrotic cells. *EMBO Rep.* 5, 825–830.
44. Messmer, D., Yang, H., Telusma, G., Knoll, F., Li, J., Messmer, B., Tracey, K.J., and Chiorazzi, N. (2004). High mobility group box protein 1: an endogenous signal for dendritic cell maturation and Th1 polarization. *J. Immunol.* 173, 307–313.
45. Ciucci, A., Gabriele, I., Percario, Z.A., Affabris, E., Colizzi, V., and Mancino, G. (2011). HMGB1 and cord blood: its role as immuno-adjuvant factor in innate immunity. *PLoS ONE* 6, e23766.
46. Chang, M.C., Chen, C.A., Hsieh, C.Y., Lee, C.N., Su, Y.N., Hu, Y.H., and Cheng, W.F. (2009). Mesothelin inhibits paclitaxel-induced apoptosis through the PI3K pathway. *Biochem. J.* 424, 449–458.
47. Chiang, Y.C., Lin, H.W., Chang, C.F., Chang, M.C., Fu, C.F., Chen, T.C., Hsieh, S.F., Chen, C.A., and Cheng, W.F. (2015). Overexpression of CHI3L1 is associated with chemoresistance and poor outcome of epithelial ovarian carcinoma. *Oncotarget* 6, 39740–39755.
48. Chang, M.C., Chen, Y.L., Chiang, Y.C., Cheng, Y.J., Jen, Y.W., Chen, C.A., Cheng, W.F., and Sun, W.Z. (2016). Anti-CD40 antibody and toll-like receptor 3 ligand restore dendritic cell-mediated anti-tumor immunity suppressed by morphine. *Am. J. Cancer Res.* 6, 157–172.

YMTHE, Volume 26

Supplemental Information

Irradiation Enhances Abscopal Anti-tumor Effects of Antigen-Specific Immunotherapy through Regulating Tumor Microenvironment

Ming-Cheng Chang, Yu-Li Chen, Han-Wei Lin, Ying-Cheng Chiang, Chi-Fang Chang, Shu-Feng Hsieh, Chi-An Chen, Wei-Zen Sun, and Wen-Fang Cheng

Supplementary Figures and Legends

Supplementary Figure 1. Alterations of CD4⁺ and CD8⁺ lymphocytes in splenocytes of

mice with tumors treated using various doses of whole-body irradiation. Representative

images (A) and bar figures (B) showing flow cytometry analysis of CD4⁺ and CD8⁺

lymphocytes at day 21 in various experimental groups: naïve (no tumor and no irradiation),

tumor + whole-body irradiation 80 cGy, tumor + whole-body irradiation 150 cGy, tumor +

whole-body irradiation 300 cGy ($n = 5$ per group). Bar figure data are shown as mean \pm SD.

Note: The percentages of CD4⁺ and CD8⁺ lymphocytes, respectively, in splenocytes at day 35

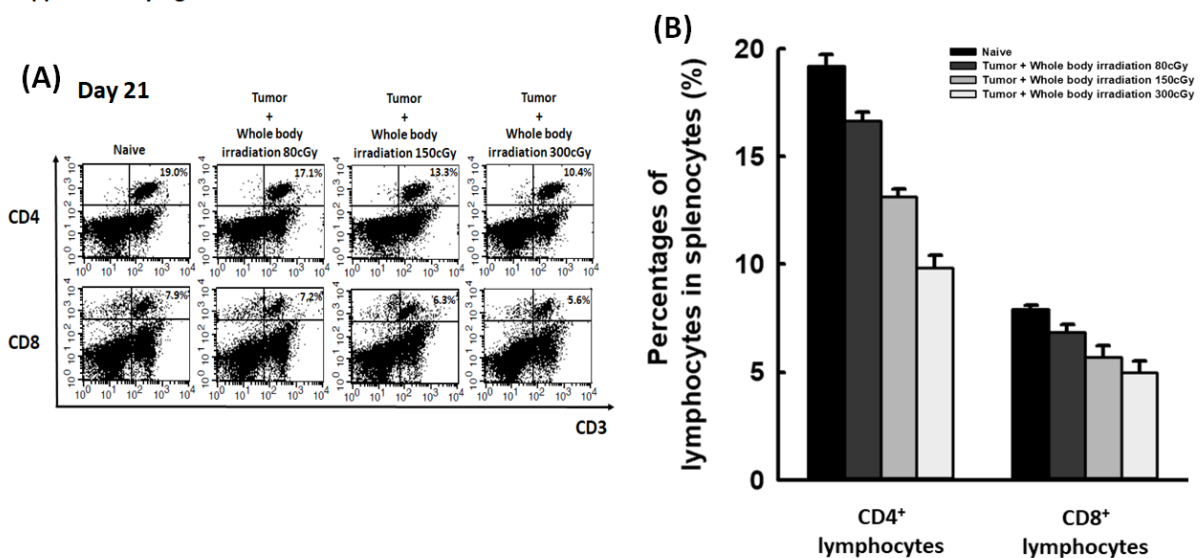
were as follows: naïve, $19.2 \pm 0.5\%$, $7.9 \pm 0.1\%$; tumor + whole-body irradiation 80 cGy,

$16.7 \pm 0.4\%$, $6.7 \pm 0.3\%$; tumor + whole-body irradiation 150 cGy, $13.1 \pm 0.4\%$, $5.7 \pm 0.5\%$;

and tumor + whole-body irradiation 300 cGy, $9.8 \pm 0.6\%$, $5.0 \pm 0.6\%$ ($P < 0.001$, $P = 0.002$,

one-way ANOVA).

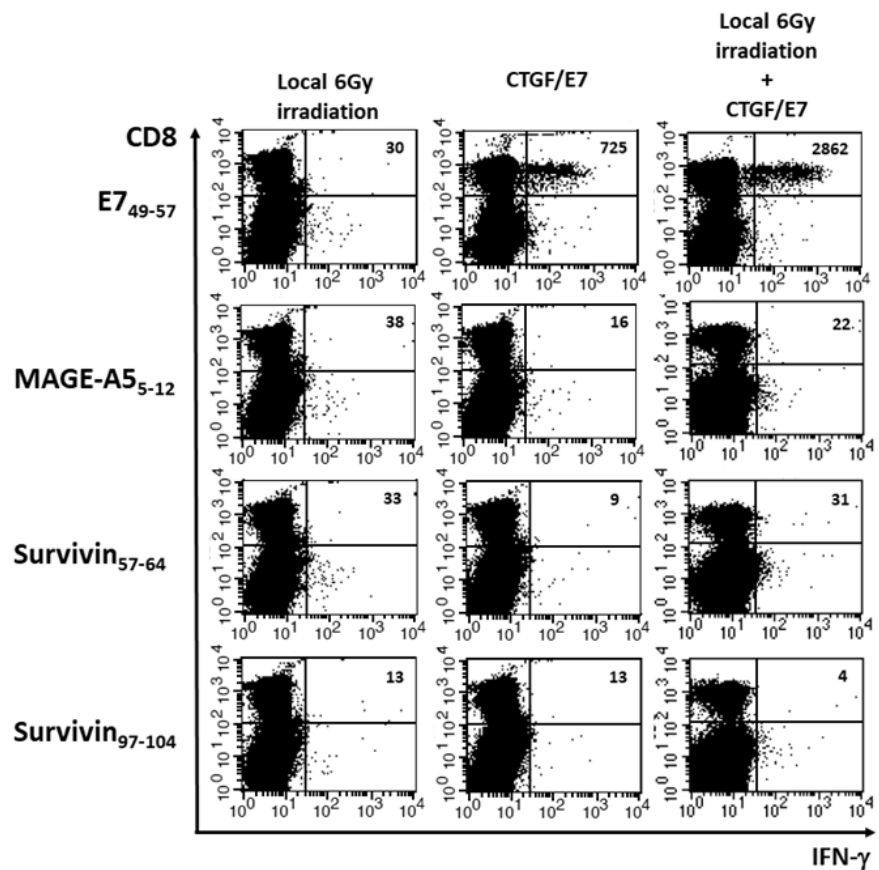
Supplementary Figure 1



Supplementary Figure 2. Antigen/epitope-specific IFN- γ -secreting CD8⁺ cytotoxic T

cells in various treatment groups. Representative figures of the flow cytometry analysis of different antigen/epitope-specific IFN- γ -secreting CD8⁺ cytotoxic T cells in various treatment groups ($n = 5$ per group). *Note:* Only E7-specific IFN- γ -secreting CD8⁺ T cells were induced in the mice treated with the CTGF/E7 DNA vaccine alone or with the CTGF/E7 DNA vaccine plus 6-Gy local irradiation.

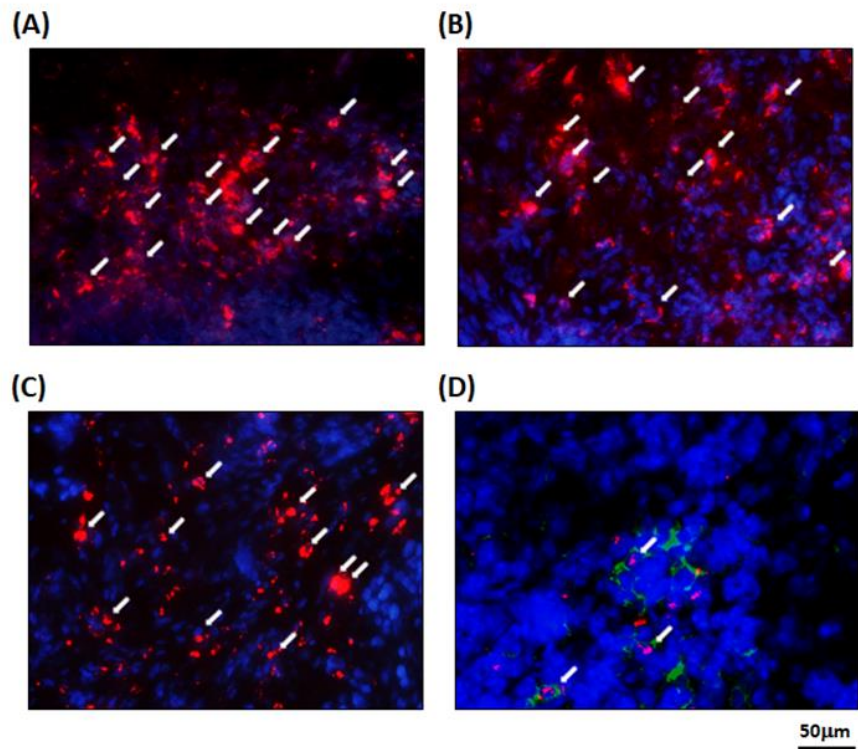
Supplementary Figure 2



Supplementary Figure 3. Other infiltrating immunocytes following treatment within

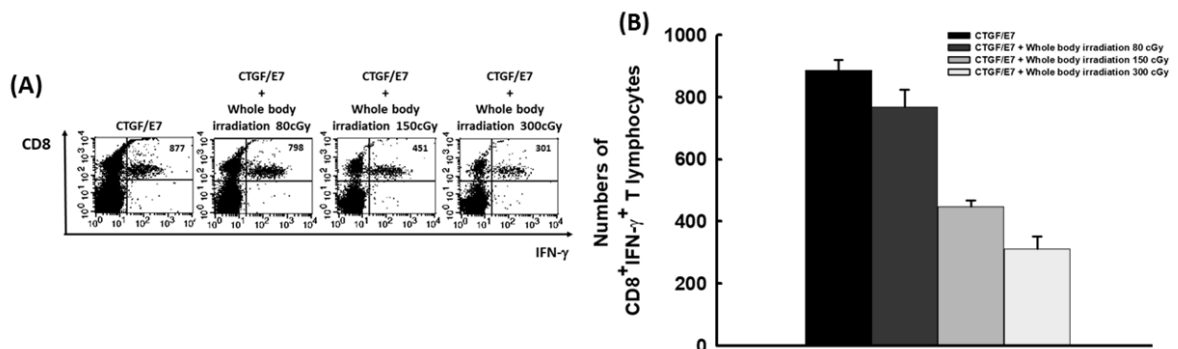
index tumors. Representative images showing immunofluorescence staining of other infiltrating immunocytes in the index tumor treated with 6-Gy local irradiation plus the CTGF/E7 DNA vaccine. A, macrophage (blue, DAPI; red, F4/80); B, neutrophil (blue, DAPI; red, Ly6g⁺); C, B lymphocytes (blue, DAPI; red, CD19); D, Tregs (blue, DAPI; red, FoxP3; green, CD4) (*n* = 5 per group).

Supplementary Figure 3



Supplementary Figure 4. The numbers of E7-specific IFN- γ -secreting CD8⁺ T cells in tumor-bearing mice treated with whole-body irradiation (overall treatment period = 2 weeks) and/or CTGF/E7 DNA vaccine. (A) Representative figures of flow cytometry analysis of the numbers of E7-specific IFN- γ -secreting CD8⁺ T cells in mice treated with whole-body irradiation and/or CTGF/E7 DNA vaccine ($n = 5$ per group). (B) Bar figures indicating the numbers of E7-specific IFN- γ -secreting CD8⁺ T cells in mice treated with whole-body irradiation and/or CTGF/E7 DNA vaccine ($n = 5$ per group). Data are shown as mean \pm SD. *Note:* The numbers of E7-specific IFN- γ -secreting CD8⁺ T cells in splenocytes were as follows: CTGF/E7, 885.1 \pm 35.1%; CTGF/E7 + whole-body irradiation 80 cGY, 767.7 \pm 55.9%; CTGF/E7 + whole-body irradiation 150 cGY, 446.3 \pm 21.0%; and CTGF/E7 + whole-body irradiation 300 cGY, 310.7 \pm 39.6% ($P < 0.001$, one-way ANOVA).

Supplementary Figure 4

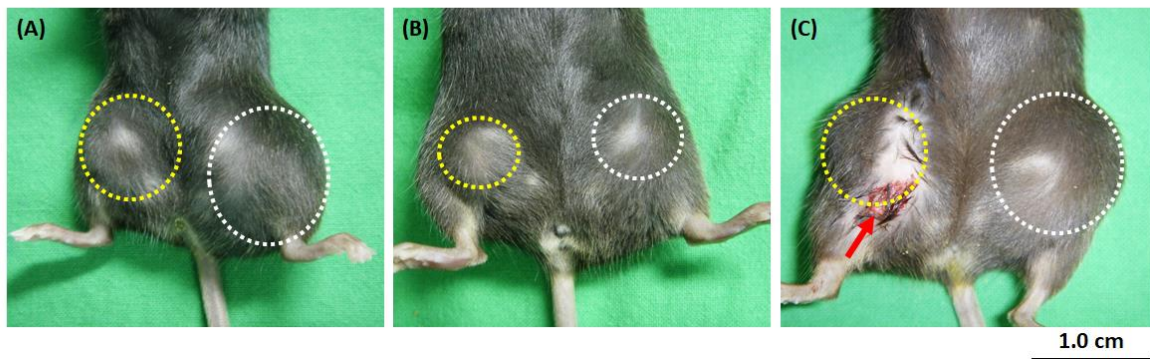


Supplementary Figure 5. Mouse index and distant tumors. Representative images

showing mouse index tumors (yellow circle, treated with DNA vaccine plus local irradiation) and distant tumors (white circle, untreated) on day 21. A, CTGF/E7 + 3-Gy local RT; B, CTGF/E7 + 6-Gy local RT; C, CTGF/E7 + 12-Gy local RT. ($n = 5$ per group). *Note:* The skin wound (red arrow) with poor healing and progression was observed starting on day 16.

Supplementary Figure 5

Day21



Supplementary Figure 6. MHC class I-expressing TC-1 tumor cells in different

treatment groups. Bar figures indicating the percentage of MHC class I-expressing TC-1

tumor cells in groups treated without or with irradiation (3, 6, or 12 Gy) at the indicated

intervals (0 and 24 h) ($n = 3$ per group). Data are shown as mean \pm SD. *Note:* The

percentages of MHC class I-expressing cells were as follows: 0-h group: 0-Gy irradiation,

$82.1 \pm 1.8\%$; 3-Gy irradiation, $81.1 \pm 1.2\%$; 6-Gy irradiation, $83.3 \pm 1.5\%$; 12-Gy irradiation,

$83.8 \pm 1.2\%$ ($P = 0.09$, one-way ANOVA); 24-h group: 0-Gy irradiation, $81.4 \pm 1.5\%$; 3-Gy

irradiation, $94.1 \pm 1.7\%$; 6-Gy irradiation, $94.6 \pm 1.6\%$; 12-Gy irradiation, $92.6 \pm 0.9\%$ ($P <$

0.001 , one-way ANOVA).

Supplementary Figure 6

